

Review

# Terpenes as Potential Anti-Alzheimer's Disease Agents

Elisabete Lima <sup>1,2</sup>  and Jorge Medeiros <sup>2,3,\*</sup> 

- <sup>1</sup> Institute of Agricultural and Environmental Research and Technology (IITAA), University of the Azores, 9700-042 Angra do Heroísmo, Portugal; elisabete.mc.lima@uac.pt
- <sup>2</sup> Department of Physics, Chemistry and Engineering (DCFQE), Faculty of Science and Technology, University of the Azores, 9500-321 Ponta Delgada, Portugal
- <sup>3</sup> Biotechnology Centre of Azores (CBA), University of the Azores, 9700-042 Angra do Heroísmo, Portugal
- \* Correspondence: jorge.mr.medeiros@uac.pt

**Abstract:** Alzheimer's disease (AD), a slowly progressive neurodegenerative disorder, is the main cause of dementia worldwide. However, currently, the approved drugs to combat AD are effective only in treating its symptoms. In fact, an efficacious treatment for this complex and multifactorial disorder remains to be discovered, demanding the urgent development of new therapeutic approaches for the disease, such as the use of bioactive secondary metabolites (SMs) from natural sources. Sessile organisms, like plants, are unable to escape from adverse environmental conditions and must therefore create their own defense. Their main defense strategy is chemical defense that includes the production of an enormously diverse array of bioactive SMs, such as terpenes and their derivatives. This largest and most diverse group of plant SMs also provide the treatment of several diseases due to their broad-spectrum bioactivities, for example, anticancer, antioxidant, and anti-inflammatory properties. Thus, the evaluation of the neuroprotective potential of terpenes is imperative. It is known that the major AD clinical indications (CIs) are extracellular senile plaques of amyloid- $\beta$  ( $A\beta$ ) protein, intracellular hyperphosphorylated tau ( $\tau$ ) neurofibrillary tangles (NFTs), uncommon neuroinflammatory response, oxidative stress, and synaptic and neuronal dysfunction. Therefore, terpenes that may decrease these CIs might be used for AD treatment. Surely, terpenes targeting more than one AD pathogenic mechanism, multi-target drug ligands (MTDLs), have the potential to become a leading AD treatment. Thus, this review analyzes, for each CI, the scaffolds of the selected terpenes leading to the highest activity.



**Citation:** Lima, E.; Medeiros, J. Terpenes as Potential Anti-Alzheimer's Disease Agents. *Appl. Sci.* **2024**, *14*, 3898. <https://doi.org/10.3390/app14093898>

Academic Editor: Alessandro Bonardi

Received: 31 March 2024

Revised: 24 April 2024

Accepted: 29 April 2024

Published: 2 May 2024



**Copyright:** © 2024 by the authors. Licensee MDPI, Basel, Switzerland. This article is an open access article distributed under the terms and conditions of the Creative Commons Attribution (CC BY) license (<https://creativecommons.org/licenses/by/4.0/>).

**Keywords:** Alzheimer's disease; multifactorial hypothesis; neuroprotective; secondary metabolites; terpenes; multi-target drug ligands (MTDLs)

## 1. Introduction

Alzheimer's disease (AD) was discovered in 1906 by Dr. Alois Alzheimer [1]. At present, around 50 million persons are estimated to suffer from dementia worldwide, and this number is expected to increase up to 150 million in 2050, as a result of the increase in life expectancy [2]. Therefore, AD remains the subject of major ongoing research.

There are two forms of AD development, called early-onset (EOAD) and late-onset (LOAD). EOAD occurs in people younger than 65 years old, and is associated with mutations in three genes, the amyloid precursor protein (APP) gene (*APP*) and the presenilin 1 and 2 genes (*PSEN1* and *PSEN2*), which are involved in the production of the amyloid- $\beta$  ( $A\beta$ ) peptides in the brain. However, most of the cases diagnosed are associated with a LOAD form that occurs after the age of 65 [3,4], and has been consistently associated, across numerous studies, with only one gene, the apolipoprotein E (ApoE) gene (*APOE*). The *APOE*  $\epsilon$ 4 allele (*APOE* $\epsilon$ 4) is a major genetic risk factor [5,6], generating cognitive dysfunction and cerebral  $A\beta$  in aged individuals [7,8]. In addition, *APOE* $\epsilon$ 4 has been associated with tau ( $\tau$ ) pathology [9]. Nevertheless, up to 75% of *APOE* $\epsilon$ 4 homozygous carriers do not

progress to AD and 50% of AD patients are not *APOE*ε4 carriers [5,6]. In fact, the genetic tendency toward LOAD and the role of other risk factors remains unclear [4].

Although the mechanisms of action of the above-mentioned genes in AD pathogenesis have been studied extensively, those involved in AD progression are still not clear, suggesting that AD is driven by a complex combination of genetic and other risk factors, such as biological and environmental factors [10]. Owing to this complexity, there is currently no cure for AD [11], and this disease is becoming a major public health concern worldwide. In fact, the action against AD has mostly focused on symptom management.

It is well established that the major clinical indications (CIs) of AD are extracellular plaques of Aβ protein, intracellular neurofibrillary tangles (NFTs) formed by hyperphosphorylated τ-protein, uncommon neuroinflammatory response, oxidative stress, and synaptic and neuronal dysfunction [12–14]. Aβ plaques may cause cell death as they interfere with the communication at synapses between neurons, while NFTs block the axonal transport with neuropathological consequences [3].

Concerning Aβ plaques, their major building blocks are Aβ peptides having a length of 40–42 amino acids, that come from the cleavage of the transmembrane protein APP by the amyloidogenic pathway, involving the action of two enzymes: β-secretase (β-site APP-cleaving enzyme 1; BACE1) and γ-secretase. APP is first cleaved by BACE1, resulting in a soluble fragment, β-APP, and a longer peptide with 99 amino acids (C99). The C99 fragment is subsequently cleaved by γ-secretase to release Aβ peptides of varying length, including Aβ-40 and Aβ-42 [15]. The Aβ generation/clearance imbalance leads to cell death. Thus, one therapeutic strategy to combat AD is preventing the appearance of brain Aβ plaques by BACE1 inhibition.

Regarding NFTs, their major constituent is a hyperphosphorylated form of τ-protein, a microtubule (MT)-binding protein. Indeed, when hyperphosphorylated, τ-protein aggregates into paired helical filaments (PHFs) and straight filaments (SFs), which result in formation of the NFTs, losing MTs that become destabilized [16–18]. MTs, crucial constituents of the eukaryotic cell cytoskeleton, are involved in several important structural and regulatory functions. These biopolymers, composed of α/β-tubulin heterodimers [18], are always vibrating, alternating between growing (polymerization) and shrinking (depolymerization) phases [19]. Due to their dynamic instability nature, MTs can change rapidly and produce a variety of different arrays within cells. The presence of different tubulin isoforms, post-translational modifications (PTMs), and interactions with MT-associated proteins (MAPs) regulates MT morphology and stability, and thus, their function in different cell types [20]. Dysfunctions in the MT system are related to the appearance of several neurodegenerative tauopathies including AD [21]. As a result, MT stabilization may also potentially prevent AD progression. AD prevention also occurs by reducing τ-protein phosphorylation, thus avoiding MT dysfunction [22,23]. Since the degree of τ-protein phosphorylation reflects a balance between the competing actions of protein kinases and phosphatases, kinase inhibitors restrain the processes of aggregation and the formation of NFTs [24–26]. Thus, another promising strategy to combat AD is the inhibition of these protein kinases [25–37]. The most important protein kinase that is involved in τ-protein phosphorylation, and thus NFT formation, is the glycogen synthetase kinase-3 beta (GSK3β) [11,15].

The inflammatory response of microglial cells is another key hallmark of AD pathology [38,39]. Microglia, the brain's resident immune cells [40], upon stimulation can convert themselves, enabling their phagocytic functions and releasing a diversity of proinflammatory factors (P-IFs), including tumor necrosis factor-α (TNF-α), interleukins 1 and 6 (IL-1 and IL-6), reactive oxygen species (ROS), nitric oxide (NO), prostaglandin E2 (PGE2), and cyclooxygenase-2 (COX-2) [41–43]. Accumulation of these P-IFs results in damage and degeneration of nearby neurons. Then, the damaged neurons release certain immune substances, increasing the inflammatory neurotoxicity and causing irreversible neuroinflammation [44–46]. Therefore, another potential therapeutic strategy to combat AD is the use of inhibitors of microglia response.

Cognitive or memory-related impairments in AD patients are associated with the deficiency of the brain neurotransmitter acetylcholine (ACh). Nevertheless, upon action of acetylcholinesterase enzyme (AChE), ACh breaks down into acetate and choline. Then, choline is up taken into the presynaptic neuron and carried out by choline carriers, and the signal transduction at the neuromuscular junction finishes rapidly [47]. AChE inhibition prevents the hydrolysis of ACh, increasing its concentration and duration of action, which is clinically beneficial for AD patients. Therefore, AChE inhibitors are widely used for the AD treatment [48]. On the other hand, ACh binds to several receptors in the synaptic cleft. One of them, the nicotinic ACh receptor (nAChR) in the central nervous system, controls the liberation of other neurotransmitters that are involved in cognitive processes and memory [48,49]. Thus, another strategy to combat AD is controlling nAChRs.

AD pathology can thus progress through different pathways which can even be related. For example, AChE accelerates A $\beta$  formation [50]. Furthermore, the interaction between AChE and A $\beta$  deposits produces the AChE–A $\beta$  complex, a very toxic substance, which in turn increases the intracellular calcium load and decreases mitochondrial membrane potential. The AChE–A $\beta$  complex formation causes neuronal cells' death [51]. AChE also stimulates the protein kinase C (PKC), which inhibits GSK3 $\beta$ . Thus, the above mechanisms may work together through interaction between genetic, molecular, and cellular events [52].

Among several strategies that have been identified to combat AD, multi-target drug ligands (MTDLs) represent an effective strategy for the treatment of this multifactorial disease, as compared to single-targeted agents and combined therapy [53]. For example, neuroinflammation and deficit of cholinergic activities are considered major contributing factors for AD. Thus, compounds that have activity against AChE and anti-inflammatory properties are multi-target compounds able to combat AD.

In the last few decades, significant research effort has been devoted to the development of anti-AD agents from natural sources (including plants, microbes, and marine organisms), which are considered to be safer and to have lesser side effects as compared to those of synthetic drugs. In fact, effective drugs approved by the Food and Drug Administration (FDA) of the United States include the AChE inhibitors galanthamine, which is a natural product itself, and rivastigmine, a semi-synthetic derivative of a natural product called physostigmine [54,55].

Among the natural products, terpenes and their derivatives, i.e., terpenes containing different functional groups (also known as terpenoids), are the largest and the most diverse group of plant secondary metabolites (SMs). Terpenes are composed of multiple isoprene units (C<sub>5</sub>H<sub>8</sub>). Nevertheless, not all terpenes have even numbers of intact isoprene units, and some of them are different, such as the C<sub>19</sub> diterpenes (nor-diterpenes) [56]. Others, such as the meroterpenes, are hybrid SMs that derive partially from the terpene pathway [57]. One of the most applied classifications for terpenes is based on the number of five-carbon units (called isoprene units) present in their chemical structure (Figure 1). Hemiterpenes have a scaffold based on one isoprene unit (C<sub>5</sub>). Monoterpenes present two isoprene units (C<sub>10</sub>) and express different arrangements, such as acyclic, monocyclic, and bicyclic. Sesquiterpenes, constituted by three isoprene units (C<sub>15</sub>), are also acyclic or mono-, di-, and tricyclic compounds. Diterpene and triterpene compounds (C<sub>20</sub> and C<sub>30</sub>, respectively) have a wide distribution from many different carbon skeletons. Tetraterpenes (C<sub>40</sub>) have a large structure, and they are also known as carotenoids [56]. Compared with the referred terpene groups, the sesterterpenes (C<sub>25</sub>) are the rarest terpene group originating from plant sources. Terpenes are biosynthesized in superior plants from two interconvertible five-carbon precursors, isopentenyl diphosphate (IPP) and its isomer dimethylallyl diphosphate (DMAPP) (Figure 1). IPP and DMAPP are generated from two alternative biosynthetic routes (Figure 1), the cytosolic acetate/mevalonate (MVA) pathway and the plastidic pyruvate/methylerythritol phosphate (MEP) pathway, also known as the non-mevalonate pathway. Terpene synthases (TPSs) are regarded as the critical catalytic enzyme along the terpene biosynthetic pathways. Moreover, the vast types of terpenes arise from the different TPS types present in the plants [54,56,58].

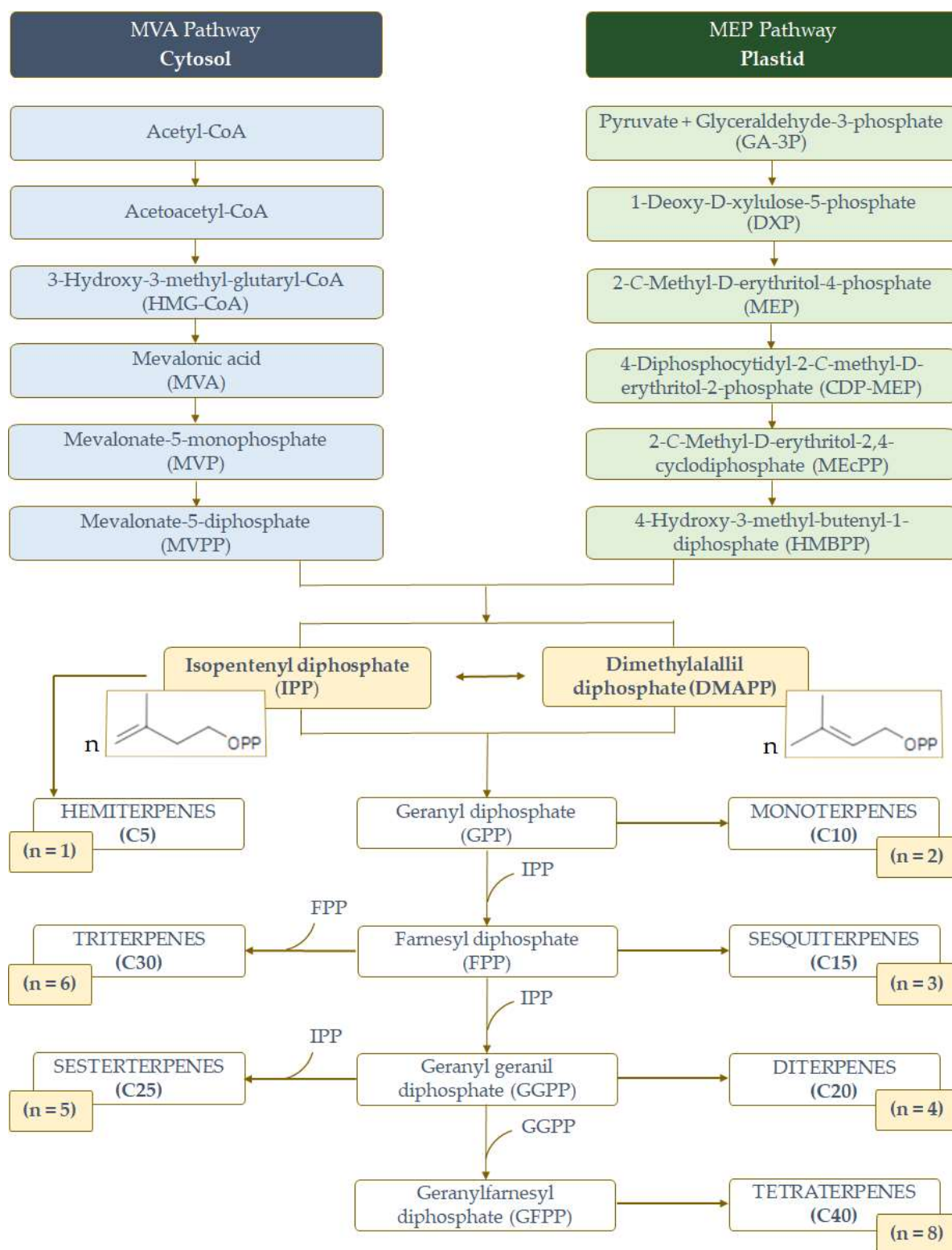


**Figure 1.** The mevalonate (MVA) and methylerythritol phosphate (MEP) pathways in biosynthesis of plant terpenes. These compounds can be classified by the number of isoprene units (n) present in the chemical structure.

Because of their chemical diversity, terpenes play many important functional roles to enhance the plant's overall fitness, thereby fostering their survival in a co-evolving ecosystem. Furthermore, these plant SMs have a widespread industrial application, ranging

from flavors and fragrances (e.g., linalool) to medicines (e.g., Taxol<sup>®</sup> and artemisinin). In fact, to date, many terpenes, mainly from essential oils and plant extracts, as well as forest bathing, have been reported to exhibit a plethora of important bioactivities ranging from antioxidant, anti-inflammatory, and anticancer to neuroprotection properties [54,55,58]. As a result, terpenes, mainly obtained from medicinal plants, have a huge potential for being novel, multi-targeted, and low-toxicity anti-AD drugs [55]. Thus, the current review focuses on the several terpenes that have been analyzed for their neuroprotective effects through the mechanisms highlighted below (Figure 2).

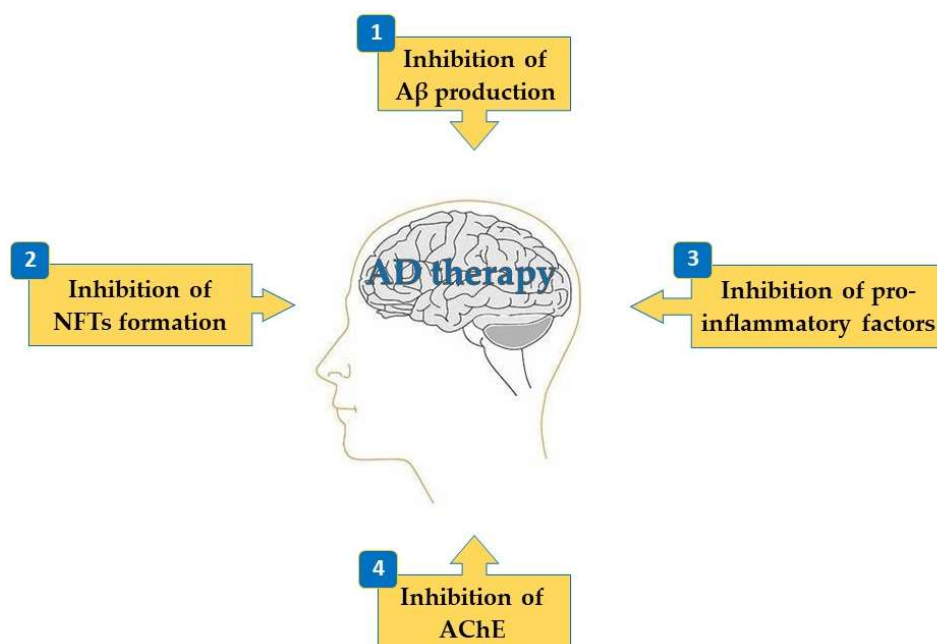


**Figure 2.** Activities of selected terpenes on mechanisms associated with Alzheimer's disease.

Our main objective is to recognize and discuss, for each CI, the scaffolds of the selected terpenes leading to the highest activity (lower  $IC_{50}$ ) and so seek those that modulate multiple targets, the MTDLs, which have the potential to become a leading AD treatment. As summarized in Table A1 and presented in Appendix A, we selected 221 terpenes. Their  $\log_{10}$  value of the octanol–water partition coefficient ( $\log P$ ) is also shown in Table A1. This constant is frequently used as a measure for the lipophilicity of a molecule, which can be used as a quick and simple prediction of its blood–brain barrier (BBB) permeability. Thus, the  $\log P$  parameter is important in the field of drug discovery, and is one criterion used in decision-making by medicinal chemists in pre-clinical drug discovery, for example, in the assessment of druglikeness of drug candidates [59–61].

Overall, the selected terpene compounds (Appendix A, Table A1), including mono-, di-, sesqui-, tri-, and tetraterpenes, as well as meroterpenes, isolated mainly from plants, were screened for their inhibition capacity of BACE1 (1–43), GSK3 $\beta$  (5), P-IFs (1, 3–6, 9, and 44–92) and AChE (1, 32–43, 47, 48, 53, 68–70, and 93–221), as described and discussed in Sections 2 and 3, respectively.

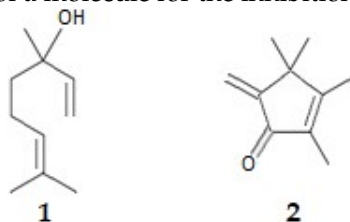
## 2. Activities of Terpenes on the Mechanisms Associated with AD

### 2.1. Inhibition of A $\beta$ Production

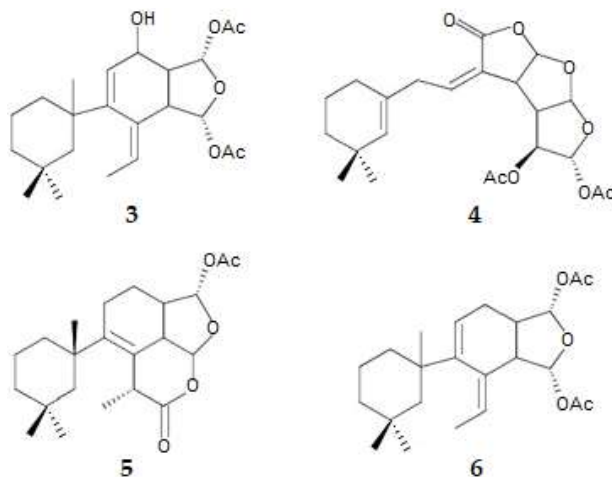
BACE1 catalyzes the rate-limiting step in the generation of A $\beta$  plaques, which plays a critical early role in AD pathogenesis, as detailed above. So, the inhibition of this enzyme reduces the load of A $\beta$  plaques in the neuronal cells by slowing or reversing the process [62]. It should also be noted that terpene compounds are characterized by low molecular weight and high hydrophobicity. Thus, they can cross cellular membranes and the BBB, an essential attribute for BACE1 inhibition in vivo [63].

### 2.1.1. Monoterpenes and Diterpenes

From the essential oil of *Lavandula luisieri* (Rozeira) Rivas-Martinez collected at Serra-do-Açor, Portugal, the monoterpenes linalool (**1**) and 2,3,4,4-tetramethyl-5-methylene-cyclopent-2-enone (**2**) were obtained. While linalool was inactive, the 2,3,4,4-tetramethyl-5-methylene-cyclopent-2-enone, an uncommon necrodane monoterpene ketone, inhibited by  $31.8 \pm 0.9\%$  recombinant proBACE1 produced in *Escherichia coli* (at a concentration of  $45 \mu\text{M}$ ). The same compound (**2**) inhibited a cell culture of Chinese hamster ovary cells (CHO) stably transfected with the APPwt coding sequence (CHO-APPwt) by  $71.4 \pm 2.5\%$  in the same concentration ( $45 \mu\text{M}$ ) [63]. These results suggest the importance of planarity of a molecule for the inhibition of BACE1.



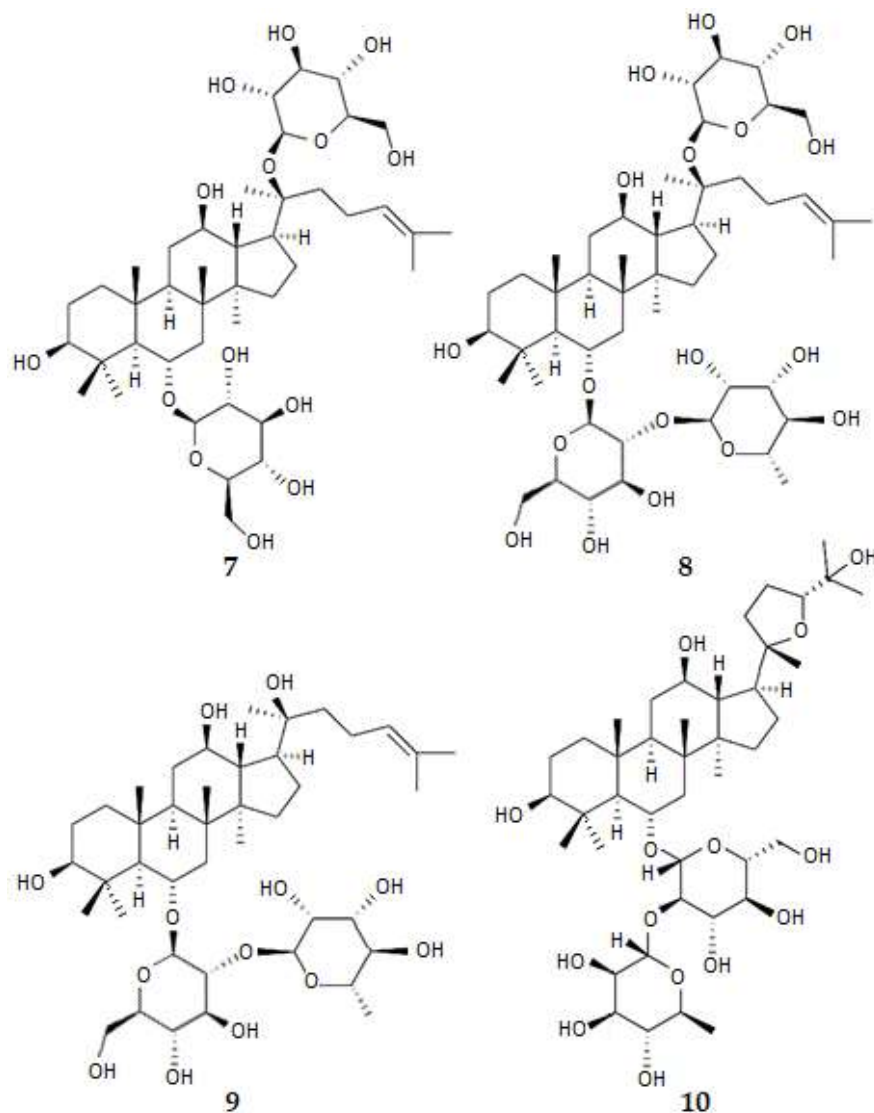
Gracilins are C<sub>19</sub> diterpenes (nor-diterpenes) which were extracted from *Spongionella gracilis* Vosmaer [64,65]. BACE1 inhibition capacity of these compounds was evaluated at 1 and 0.1  $\mu\text{M}$  with the BACE1 FRET assay kit [65]. Gracilin L (**3**) ([*(1S,3R,3aR,4Z,7S,7aS)*-3-acetyloxy-4-ethylidene-7-hydroxy-5-[(*1S*)-1,3,3-trimethylcyclohexyl]-3,3a,7,7a-tetrahydro-1*H*-2-benzofuran-1-yl] acetate) at 1  $\mu\text{M}$  produced inhibition of BACE1, decreasing its activity by  $24.6 \pm 4.2\%$ . Gracilin H (**4**) and tetrahydroaplysulphurin-1 (**5**) also presented activity but lower than the one presented by compound **3**, while gracilin A (**6**), the [*(1S,3R,3aR,4Z,7aR)*-4-ethylidene-5-[(*1S*)-1,3,3-trimethylcyclohexyl]-1,3,3a,4,7,7a-hexahydro-2-benzofuran-1,3-diyl] diacetate, was inactive. It is interesting to note that gracilin L (**3**) is the only compound of this series that presents a polar hydroxyl group at C7 and can present an almost planar conformation.



### 2.1.2. Triterpenes and Meroterpenes

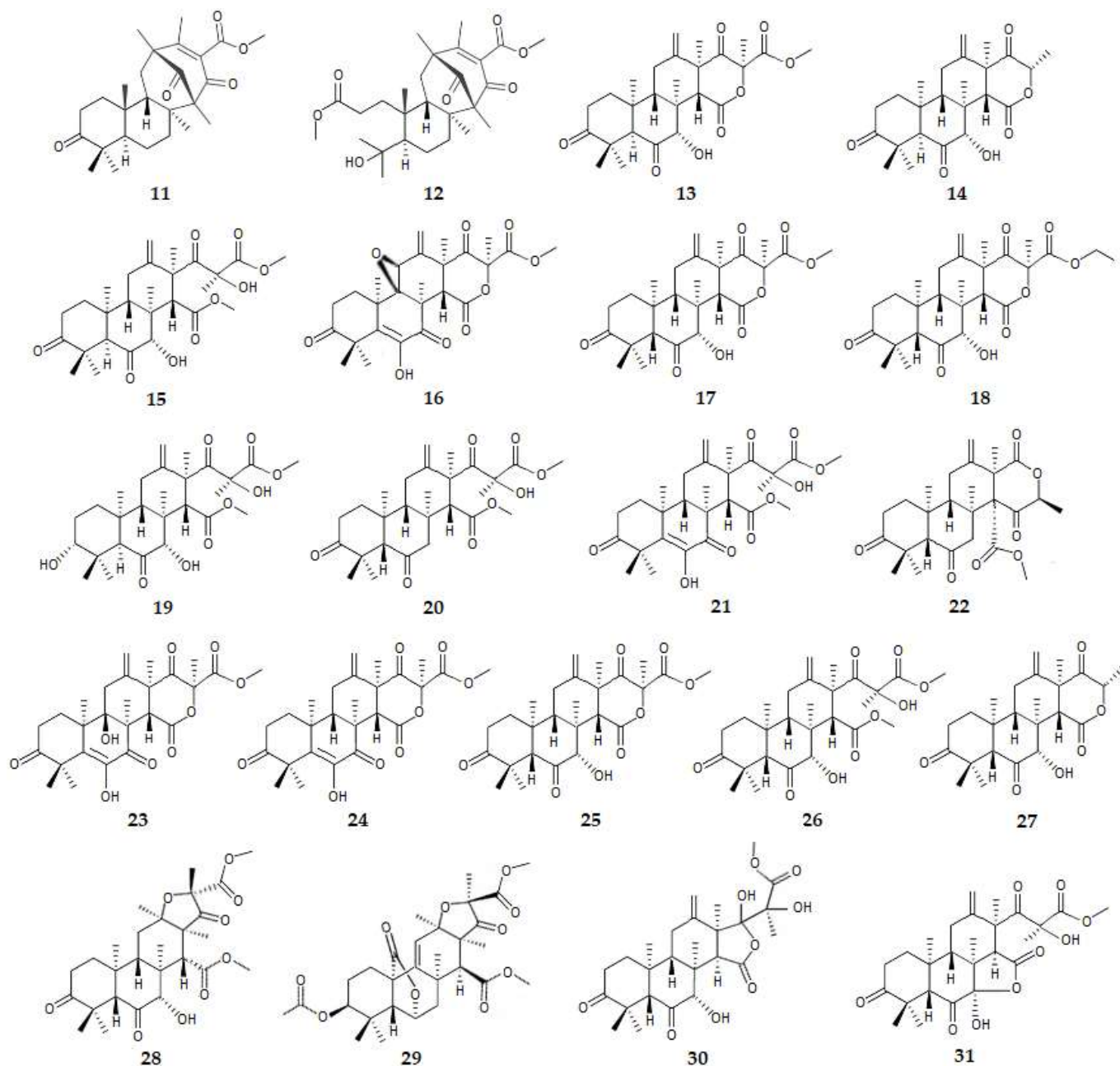
From *Panax ginseng* C.A. Meyer from China, as well as from other species of ginseng, ginsenosides were extracted. These compounds are steroidal triterpene saponins with the usual four rings (A, B, C, and D) of the steroid backbone [64]. Ginsenoside Rg1 (**7**) presented a BACE1 IC<sub>50</sub> value of  $6.18 \pm 0.96 \mu\text{M}$  [64,66]. Ginsenoside Re (**8**) also presented some activity as a BACE1 inhibitor; however, the IC<sub>50</sub> value was not determined [64,67]. These ginsenosides Rg1 (**7**) and Re (**8**), as well as Rg3 (**9**), significantly reduce the amount of A $\beta$ 40/A $\beta$ 42 [64,68].

Pseudoginsenoside-F11 (PF11) (**10**), an ocotillol-type saponin contained in *Panax quinquefolium* L. and isolated from leaves of *Panax pseudoginseng* Wall. subsp. *Himalaicus* HARA (Himalayan ginseng), suppresses the expression of BACE1 [69,70].

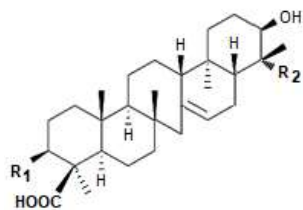


Meroterpenes are hybrid SMs that derive partially from the terpene pathway [57]. Biosynthetically, the complex structures of these compounds are mostly derived from simple precursors like a linear isoprene or a C-2 unit like acetyl-CoA, via several chemical transformations [71,72]. The meroterpenes asperterpenes, extracted from the mold *Aspergillus terreus* Thom., showed BACE1 inhibitory activities. The asperterpenes A (11), B (12), E (13), F (14), and J (15) presented  $IC_{50}$  values of 0.08, 0.06, 3.32, 5.85, and 31.68  $\mu\text{M}$ , respectively [73,74]. However, other asperterpenes like D (16), G (17), H (18), I (19), K (20), L (21), or M (22) were inactive ( $IC_{50} > 50 \mu\text{M}$ ) [73,74]. Other meroterpenes like terretonin (23) or terretonins A (24), D (25), G (26), and H (27) were also inactive ( $IC_{50} > 50 \mu\text{M}$ ) [74]. These results suggest that in asperterpenes A (11) and B (12), the unique  $\beta$ -oriented methyl group at C21 with the unprecedented 1,2,5-trimethyl-4,9-dioxobicyclo[3.3.1]non-2-ene-3-carboxylic acid moiety, and in asperterpenes E (13) F (14) and J (15) the cis-fused A/B rings, are important for BACE1 inhibition activity [64,73].

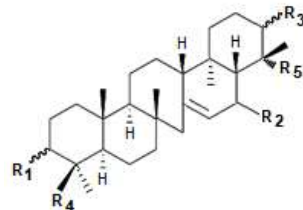
Considering the terreusterpenes, another series of 3,5-dimethylorsellinic acid-based meroterpenes also obtained from *A. terreus*, some of them showed high BACE1 inhibition activity. Terreusterpenes A (28), B (29), C (30), and D (31) inhibited the activity of BACE1 with  $IC_{50}$  values of 5.98, 11.42, >40, and 1.91  $\mu\text{M}$ , respectively [75]. These results suggest that the 4-hydroxy-3 methyl  $\gamma$  lactone fragment of terreusterpene D (31), making a more planar molecule, is important for the inhibition of BACE1.



From *Lycopodiella cernua* L., with synonyms of *Lycopodium cernuum* L., *Lepidotis cernua* (L.) P. Beauv., or *Pallinhaea cernua* (L.) Pic. Ser., of Vietnam, twelve serratene-type pentacyclic triterpenes (compounds **32–43**) were isolated. While compounds 3 $\beta$ ,21 $\beta$ ,29-trihydroxyserrat-14-en-24-oic acid-3 $\beta$ -yl-(70-hydroxycinnamate) (**32**), 3 $\beta$ ,14 $\alpha$ ,15 $\alpha$ ,21 $\beta$ -tetrahydroxyserrat-24-oic acid-3 $\beta$ -yl-(40-methoxy-50-hydroxybenzoate) (**33**), 3 $\beta$ ,21 $\beta$ ,29-trihydroxyserrat-14-en-24-oic acid-3 $\beta$ -yl-(40-hydroxybenzoate) (**35**), and 21 $\beta$ -hydroxyserrat-14-en-3,16-dione (**36**) were active as BACE1 inhibitors with IC<sub>50</sub> values of 1.07, 1.0, 0.3, and 0.2  $\mu$ M, respectively, all the other compounds were inactive (IC<sub>50</sub> > 10  $\mu$ M). They were identified as 3 $\beta$ ,21 $\beta$ ,29-trihydroxyserrat-14-en-3 $\beta$ -yl *p*-dihydrocoumarate (**34**), 3 $\beta$ ,21 $\alpha$ -diacetoxyserrat-14 $\beta$ -ol (**37**), serrat-14-en-3 $\alpha$ ,21 $\alpha$ -diol (**38**), 3 $\beta$ ,21 $\beta$ ,29-trihydroxy-16-oxoserrat-14-en-24-oic acid (**39**), serrat-14-en-3 $\alpha$ ,21 $\beta$ -diol (**40**), 3 $\beta$ ,21 $\beta$ ,29-trihydroxy-16-oxoserrat-14-en-24-methyl ester (**41**), 3 $\beta$ ,21 $\alpha$ -dihydroxyserrat-14 $\beta$ -ol (**42**), and 3 $\alpha$ ,21 $\beta$ -dihydroxy-16-oxoserrat-14-en-24-oic acid (**43**) [76]. Compound **36** is the most potent as a BACE1 inhibitor, suggesting that the conjugated system comprising the double bond between C14 and C15 and the carbonyl group of C16, making the ring more planar, is important for inhibition.



- 32  $R_1 = p$ -hydroxycinnamoyl;  $R_2 = CH_2OH$   
 33  $R_1 = 4'$ -methoxy-5'-hydroxybenzoyl;  
 $R_2 = CH_3, 14\alpha-OH, 15\alpha-OH$   
 34  $R_1 = p$ -dihydrocoumaroyl;  $R_2 = CH_2OH$   
 35  $R_1 = p$ -hydroxybenzoyl;  $R_2 = CH_3, 14\alpha-OH, 15\alpha-OH$



- 36  $R_1 = O; R_2 = O; R_3 = \beta-OH; R_4 = CH_3; R_5 = CH_3$   
 37  $R_1 = \beta-OAc; R_2 = 14\beta-OH; R_3 = \alpha-OAc; R_4 = CH_3; R_5 = CH_3$   
 38  $R_1 = \alpha-OH; R_2 = H,H; R_3 = \alpha-OH; R_4 = CH_3; R_5 = CH_3$   
 39  $R_1 = \beta-OH; R_2 = O; R_3 = \beta-OH; R_4 = COOH; R_5 = CH_2OH$   
 40  $R_1 = \alpha-OH; R_2 = H,H; R_3 = \beta-OH; R_4 = CH_3; R_5 = CH_3$   
 41  $R_1 = \beta-OH; R_2 = O; R_3 = \beta-OH; R_4 = COOCH_3; R_5 = CH_2OH$   
 42  $R_1 = \beta-OH; R_2 = H,H; R_3 = \alpha-OH; R_4 = CH_3; R_5 = CH_3$   
 43  $R_1 = \alpha-OH; R_2 = O; R_3 = \beta-OH; R_4 = COOH; R_5 = CH_3$

## 2.2. Inhibition of NFTs Formation

### 2.2.1. Inhibition of GSK-3 $\beta$

#### Diterpenes

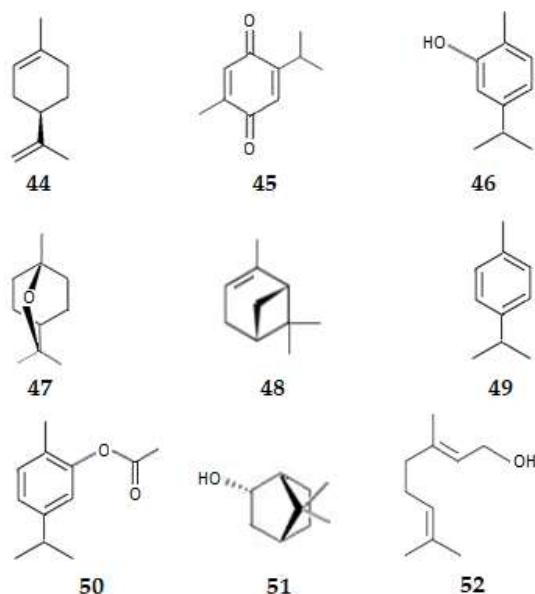
The nor-diterpenes gracilins (3–6), besides showing inhibition of BACE1, are also inhibitors of  $\tau$  phosphorylation. Using the SH-SY5Y human neuroblastoma  $\tau$  441 cellular line (SH-SY5Y-TMHT441), the inactive isoform of GSK3 $\beta$  was measured. Only tetrahydroaplysulphurin-1 (5) increased the levels of it ( $57.1 \pm 24.75\%$ ) at 0.1  $\mu$ M [65].

## 2.3. Inhibition of Pro-Inflammatory Factors

### 2.3.1. Monoterpenes

ROS production in AD flies fed with (+)-limonene (44) is reduced significantly, which means that (+)-limonene (44) has antioxidant activity not only in vitro, but also in vivo. That antioxidative activity has anti-inflammatory effects and so there is a reduced inflammatory response in this *Drosophila* model of AD after (+)-limonene (44) is ingested [77]. Linalool (1), existing in several plants and extracted by hydrodistillation, decreases the levels of ROS significantly when a concentration of 400  $\mu$ M is used. It also decreases the levels of NO significantly [78,79]. Thymoquinone (45) extracted from *Nigella sativa* L. [80], inhibits the production of TNF- $\alpha$  and IL-1 $\beta$  [81]. It crosses the BBB smoothly [82]. Carvacrol (46), existing in several plants, improves the in vivo and in vitro neuronal impairment induced by ethanol via the antioxidative and antiapoptotic pathways [83]. 1,8-Cineol (47) and  $\alpha$ -pinene (48) are other monoterpenes that show an in vitro neuroprotective activity against the H<sub>2</sub>O<sub>2</sub>-induced oxidative stress in PC12 (rat pheochromocytoma) cells. Pretreatment with these monoterpenes was found to attenuate the loss of cell viability and the changes in cell morphology. Moreover, they inhibited the intracellular ROS production [78,84]. *p*-Cymene (49), another monoterpene existing in several plants, decreases the lipid peroxidation and nitrite content of the hippocampus of Swiss mice [78,85].

The oxidative pathways seem to be regulated by the nuclear factor erythroid 2-related factor 2 (Nrf2) as an upstream mediator [78]. Carvacryl acetate (50), borneol (51), and geraniol (52), other monoterpenes existing in several plants, show neuroprotective effects against the cognitive deficits by enhancing the activity of antioxidant enzymes and up-regulating Nrf2 [78,86–88].



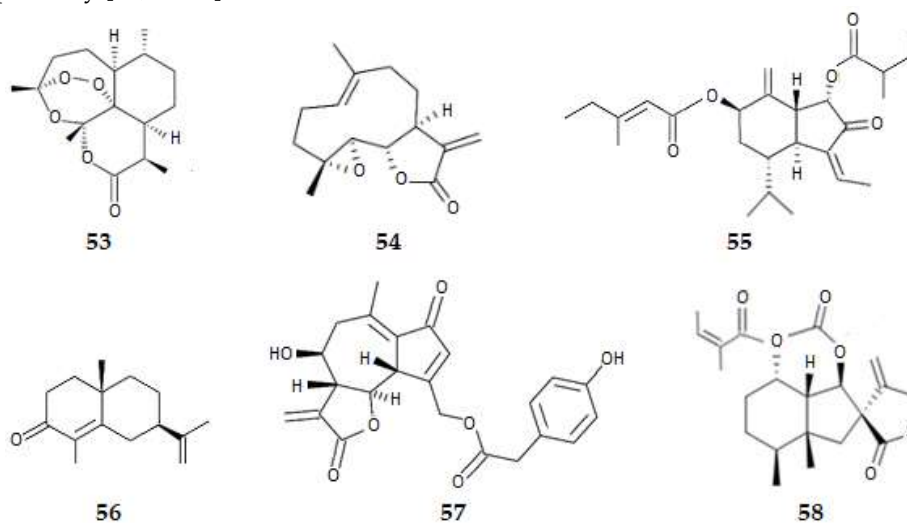
### 2.3.2. Sesquiterpenes

Artemisinin (**53**), a sesquiterpene extracted from *Artemisia annua* L., inhibits the release of TNF- $\alpha$ , IL-1 $\beta$ , IL-6, TNF- $\alpha$ , and NO [89]. It is a lipid soluble substance that readily penetrates the BBB into the brain [89]. Nevertheless, the neurotoxicity of this natural product might be an obstacle for further use in clinical research [80].

Parthenolide (**54**), another sesquiterpene existing in *Chrysanthemum morifolium* L. Bernh. [90], can inhibit the production of IL-6, TNF- $\alpha$ , and ROS [91–93].

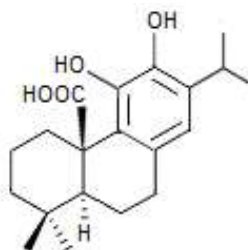
The sesquiterpene 7 $\beta$ -(3-ethyl-cis-crotonoyloxy)-1 $\alpha$ -(2-methylbutyryloxy)-3,14-dehydro-Z-notonipetranone (ECN) (**55**), isolated from *Tussilago farfara* L. widespread in East Asia, exhibits neuroprotective effects against oxidative stress-induced cell damage and dopaminergic neurodegeneration. Its mechanism of action is through potential activation of the Nrf2/antioxidant response element (ARE) signaling pathway and decreasing ROS generation in vitro and in vivo [78,91].

$\alpha$ -Cyperone (**56**), one of the main components of *Cyperus rotundus* L. essential oil, lactucopicrin (**57**) from *Lactuca virosa* L. (wild lettuce), *Cichorium intybus* L. and dandelion coffee, and bakkenolide B (**58**), extracted from *Petasites japonicus* (Siebold & Zucc.) Maxim. leaves from East Asia, ameliorate the oxidative stress by activation of the Nrf2 pathway [78,92–94].

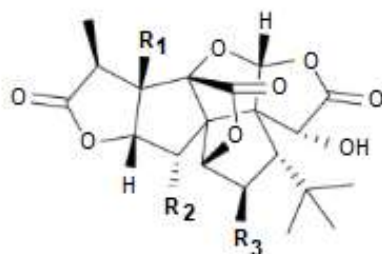


### 2.3.3. Diterpenes

Carnosic acid (**59**) is a diterpene extracted from rosemary (*Rosmarinus officinalis* L.) [89]. It also readily penetrates the BBB into the brain [95]. It reduces the production of inflammatory mediators like TNF- $\alpha$ , IL-1 $\beta$ , IL-6, and NO [96]. Other diterpenes like the ginkgolides A (**60**), B (**61**), and C (**62**) isolated from the leaves of *Ginkgo biloba* L. inhibit the production of IL-1 $\beta$  and TNF- $\alpha$  [97–99]. However, these compounds have difficulty entering the brain through the BBB [100].



**59**



**60**  $R_1 = \text{OH}; R_2 = \text{H}; R_3 = \text{H}$

**61**  $R_1 = \text{OH}; R_2 = \text{OH}; R_3 = \text{H}$

**62**  $R_1 = \text{OH}; R_2 = \text{OH}; R_3 = \text{OH}$

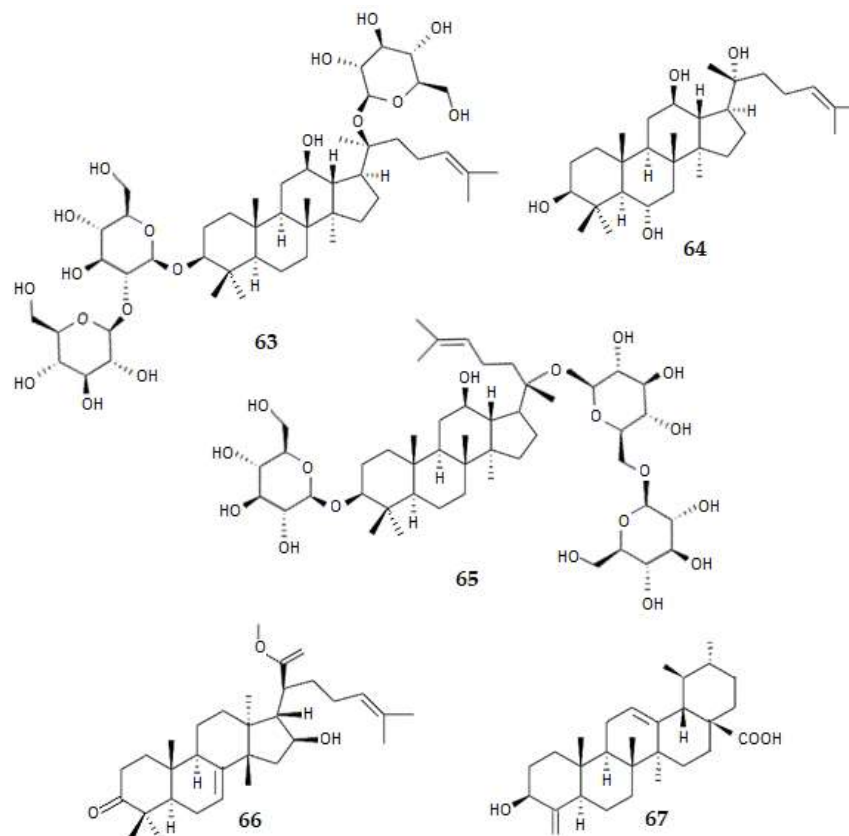
Considering the nor-diterpenes (3–6), besides BACE1 and  $\tau$  phosphorylation inhibitors, all of them reduce the production of ROS [101].

### 2.3.4. Triterpenes

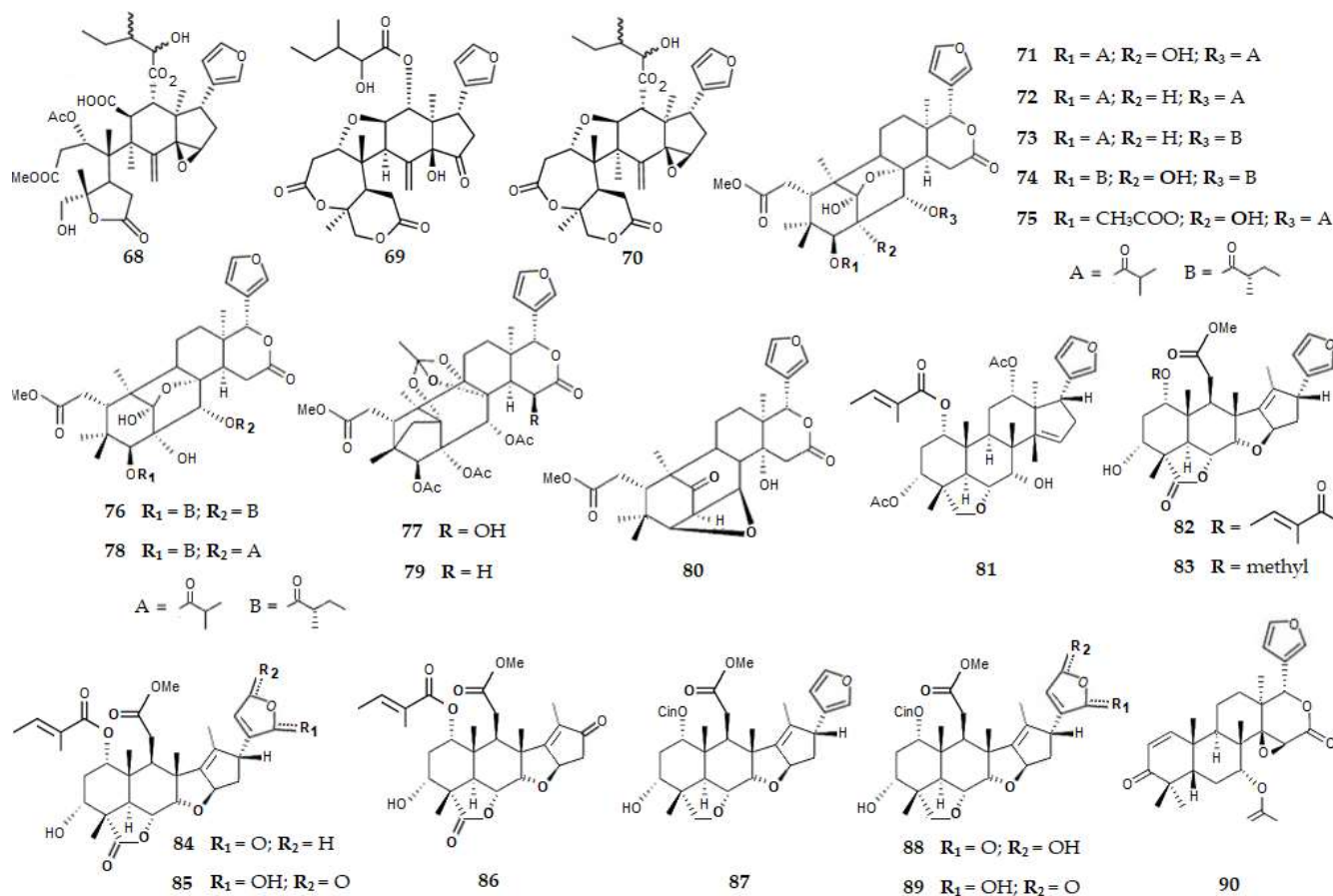
The triterpene ginsenoside Rg3 (**9**) from *P. ginseng*, significantly reduces the production of TNF- $\alpha$ , IL-1 $\beta$ , and COX-2 [102–104]. Ginsenoside Re (**8**) and ginsenoside Rg1 (**7**) are other ginsenosides exhibiting strong neuroprotective activity by inhibiting ROS and activating Nrf2 antioxidant pathways [78,105–107]. Other ginsenosides like ginsenoside Rd (**63**) and protopanaxatriol (PPT) (**64**) also exhibit neuroprotective effect by activating Nrf2 [78,108,109]. These molecules with 30 carbon atoms can easily penetrate the BBB into the brain tissue [110]. Other triterpene glycosides, with different scaffolds, such as gypenoside XVII (**65**), isolated from *Gynostemma pentaphyllum* (Thunb.) Makino, from China, exhibits neuroprotective activity by activating Nrf2 antioxidant pathways [78,111].

From the bark of *Melia azedarach* L., indigenous to Southeast Asia, the triterpene methyl kulonate (methyl 3-oxo-16 $\beta$ -hydroxyeupha-7,24-dien-21-oate) (**66**) was isolated. This triterpene exhibits potent inhibitory activity against NO production from LPS-activated macrophages with an IC<sub>50</sub> value of 4.6  $\mu\text{M}$  [112].

The triterpene 3 $\beta$ -hydroxy-24-nor-urs-4(23),12-dien-28-oic acid (**67**), extracted from *Patrinia scabiosaefolia* Fisch from China, exhibits inhibitory activity against NO with IC<sub>50</sub> value of 10.1  $\mu\text{M}$  [113].

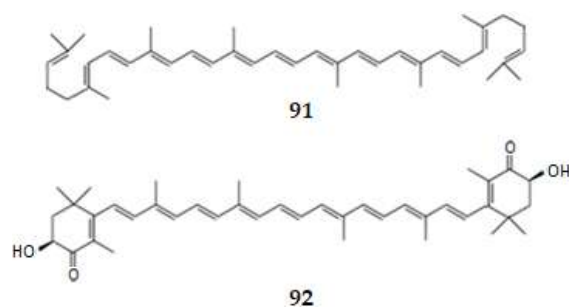


Limonoids are highly oxygenated triterpenes existing mostly in the *citrus* genus, as well as in other plant families, such as Meliaceae. Three limonoids were extracted from the seeds of *Trichilia welwitschia* C.DC. existing in Nigeria, Gabon, Angola, and Cameroon, Africa. They were identified as trichilia lactone D5 (**68**), rohituka 3 (**69**), and dregeanin DM4 (**70**). At the lowest concentration of 0.5  $\mu\text{g}/\text{mL}$ , compounds **69** and **70** release the lowest amount of NO with  $\text{IC}_{50}$  values of 2.97 and 2.93  $\mu\text{M}$ , respectively, while trichilia lactone D5 (**68**) with the same concentration releases an amount of NO above 4.0  $\mu\text{M}$  [114,115]. Ten other limonoids were extracted from the seeds of *Xylocarpus rumphii* (Kostel.) Mabb. from Thailand. They were identified as 2-hydroxyxylorumphiin F (**71**), E (**72**), F (**73**), G (**74**), H (**75**), I (**76**), and J (**77**), and the xylocensins X (**78**), E (**79**), and K (**80**). While xylorumphiin I (**76**) and 2-hydroxyxylorumphiin F (**71**) exhibit a moderate inhibitory activity against NO production from LPS-activated macrophages with  $\text{IC}_{50}$  values of 31.3 and 24.5  $\mu\text{M}$ , respectively, all the other compounds do not show any significant effects at a concentration of 50  $\mu\text{M}$  [116]. Nine other limonoids were isolated from the leaves of *M. azedarach* indigenous to Japan, Taiwan, China, India, and Southeast Asia, namely, trichilin B (**81**), 3-deacetyl-28-oxosalannin (**82**), 3-deacetyl-4'-demethyl-28-oxosalannin (**83**), 3-deacetyl-28-oxosalannolactone (**84**), 3-deacetyl-28-oxoisosalanninolide (**85**), 3-deacetyl-17-defurano-17,28-dioxosalannin (**86**), ohchinin (**87**), 23-hydroxyohchininolide (**88**), and 21-hydroxyisohchininolide (**89**). Trichilin B (**81**) and ohchinin (**87**) exhibit potent inhibitory activities toward NO production, induced by lipopolysaccharides (LPSs), by murine macrophage-derived RAW264.7 cells, with  $\text{IC}_{50}$  values of 29.2 and 28.7  $\mu\text{M}$ , respectively. 3-Deacetyl-28-oxosalannolactone (**84**), 23-hydroxyohchininolide (**88**), and 21-hydroxyisohchininolide (**89**) also exhibit inhibitory activities with  $\text{IC}_{50}$  values of 86.0, 58.6, and 87.3  $\mu\text{M}$ , respectively. All the others were inactive toward NO production ( $\text{IC}_{50} > 100 \mu\text{M}$ ) [112]. Another triterpene, gedunin (**90**), found in the seeds of *Azadirachta indica* A. Juss. (neem), from Southeast Asia, exhibits neuroprotective activity by activating Nrf2 antioxidant pathways [78,117].



### 2.3.5. Tetraterpenes

The carotenoid lycopene (91), which is a red plant pigment found in fruits such as tomatoes, watermelons, and apricots, exhibits neuroprotective activity by activating Nrf2 antioxidant pathways [78,118]. Another carotenoid, astaxanthin (92), isolated from green microalgae *Haematococcus pluvialis* Flotow, existing in Scandinavia, exhibits neuroprotective activity by activating the Nrf2/ARE signaling pathway and decreasing ROS generation [78,119,120].

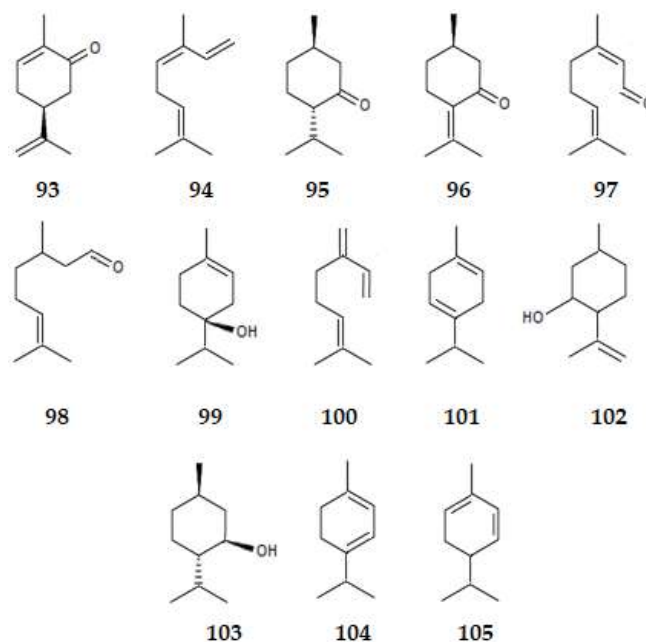


## 2.4. Inhibition of Acetylcholinesterase (AChE)

### 2.4.1. Monoterpenes

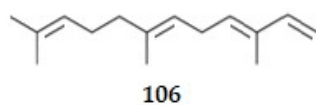
From the essential oils of several plants, many monoterpenes are obtained, such as carvone (93), ocimene (94), menthone (95), and pulegone (96). These four monoterpenes are weak inhibitors of AChE with  $IC_{50}$  values of 2900, 4700, 9000, and 9000  $\mu M$ , respectively. All the other monoterpenes, such as linalool (1), 1,8-cineol (47),  $\alpha$ -pinene (48), *p*-cymene (49), citral (97), citronellal (98), terpinene-4-ol (99),  $\beta$ -myrcene (100),  $\gamma$ -terpinene (101), isopulegol (102), menthol (103),  $\alpha$ -terpinene (104), and  $\alpha$ -phellandrene (105) are inactive

against AChE ( $IC_{50} > 10.000 \mu M$ ) [121]. These results suggest that the compounds with a carbonyl group in a cyclic monoterpene present some activity.

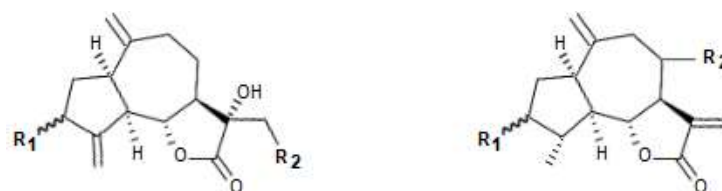


#### 2.4.2. Sesquiterpenes

Farnesene (**106**), also found in essential oils of several plants, revealed high AChE inhibitory activity in a Marston assay [121].



Cornigeraline A (**107**), a chlorinated sesquiterpene lactone, extracted from wild artichoke (*Cynara cornigera* L.) native to the Mediterranean region, northwestern Africa, and the Canary Islands, presents an  $IC_{50}$  value of  $20.5 \mu M$  as an inhibitor of AChE [114,122]. From the same plant, sibthorpine (**108**), 3-hydroxy-grosheimin (**109**), grosheimin (**110**), solstitialin A (**111**), 13-chlorosolstitialin (**112**), and cynaropicrin (**113**) also presented AChE inhibition with  $IC_{50}$  values of 35.8, 30.5, 61.8, 25.7, 62.1, and  $31.3 \mu M$ , respectively [114]. Cornigeraline A (**107**) is the most active, suggesting that the chlorine atom is important for the inhibition of AChE; however, when it is compared with its epimer, 13-chlorosolstitialin (**112**), the activity of the latter decreases 3-fold. As cornigeraline A (**107**) possess two hydrophobic moieties located in the sesquiterpene nucleus, which is close to C10 and between C1 and C3, it might pass through the BBB.



107  $R_1 = \alpha\text{-OH}$ ;  $R_2 = \text{Cl}$

108  $R_1 = \alpha\text{-OH}$ ;  $R_2 = \text{OH}$

111  $R_1 = \beta\text{-OH}$ ;  $R_2 = \text{OH}$

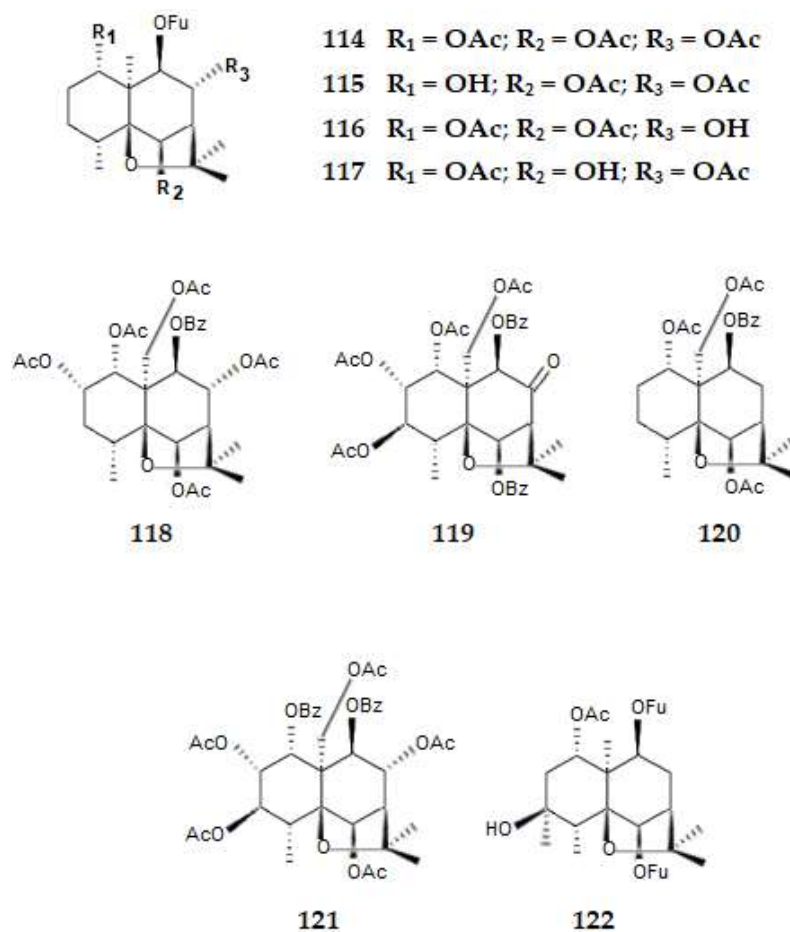
112  $R_1 = \beta\text{-OH}$ ;  $R_2 = \text{Cl}$

109  $R_1 = \beta\text{-OH}$ ;  $R_2 = \alpha\text{-OH}$

110  $R_1 = \text{O}$ ;  $R_2 = \alpha\text{-OH}$

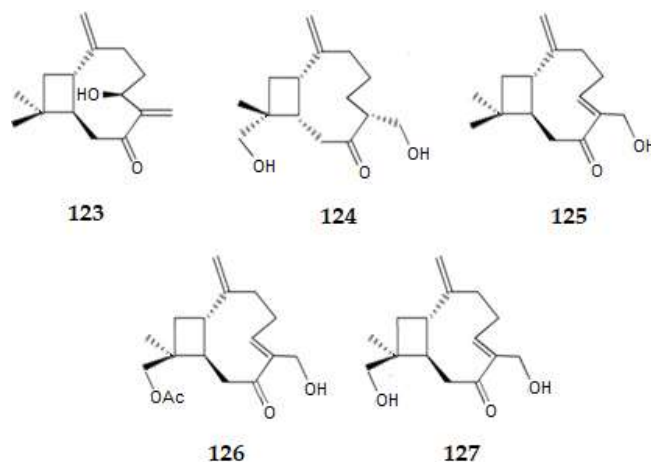
113  $R_1 = \beta\text{-OH}$ ;  $R_2 = \alpha\text{-A}$      $\text{A} = \text{O}-\text{C}(\text{O})-\text{CH}=\text{CH}-\text{OH}$

Sesquiterpenes with a dihydro- $\beta$ -agarofuran skeleton were isolated from aerial parts and seeds of *Maytenus disticha* (Hook F.) at Chile. They were identified as 1 $\alpha$ ,6 $\beta$ ,8 $\alpha$ -triacetoxy-9 $\beta$ -furoyloxy- $\beta$ -agarofuran (**114**), 1 $\alpha$ -hydroxy-6 $\beta$ ,8 $\alpha$ -diacetoxy-9 $\beta$ -furoyloxy- $\beta$ -agarofuran (**115**), 1 $\alpha$ ,6 $\beta$ -diacetoxy-8 $\alpha$ -hydroxy-9 $\beta$ -furoyloxy- $\beta$ -agarofuran (**116**), 1 $\alpha$ -acetoxy-6 $\beta$ ,8 $\alpha$ -dihydroxy-9 $\beta$ -furoyloxy- $\beta$ -agarofuran (**117**), 1 $\alpha$ ,2 $\alpha$ ,6 $\beta$ ,8 $\alpha$ -pentaacetoxy-9 $\beta$ -benzoyloxy- $\beta$ -agarofuran (**118**), 1 $\alpha$ ,2 $\alpha$ ,3 $\beta$ ,15-tetraacetoxy-6 $\beta$ ,9 $\beta$ -dibenzoyl-8-oxo- $\beta$ -agarofuran (**119**), 1 $\alpha$ ,6 $\beta$ ,15-triacetoxy-9-benzoyloxy- $\beta$ -agarofuran (**120**), 2 $\alpha$ ,3 $\beta$ ,6 $\beta$ ,8 $\alpha$ ,15-pentaacetoxy-1 $\alpha$ ,9 $\beta$ -benzoyloxy- $\beta$ -agarofuran (**121**), and 1 $\alpha$ -acetoxy,6 $\beta$ ,9 $\beta$ -difuroyloxy-4 $\beta$ -hydroxy- $\beta$ -agarofuran (**122**). The IC<sub>50</sub> values for the inhibition of AChE were 248, 738, 161, 312, 122, 463, 695, 482, and 738  $\mu$ M, respectively. These results show that these compounds are weak but selective inhibitors of AChE [114,123].

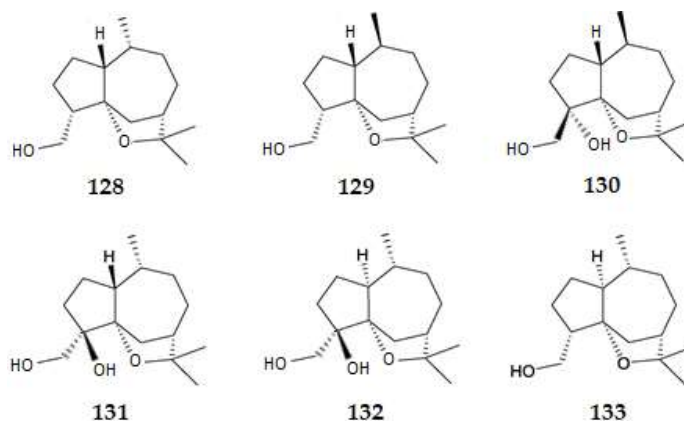


Five caryophyllene-type sesquiterpenes (compounds **123**–**127**) were isolated from the aerial parts of *Pulicaria vulgaris* Gaertn. collected at Monastir (Tunisia). While compounds (1*S*,5*Z*,9*R*,11*S*)-12,14-dihydroxycaryophylla-2(15),5-dien-7-one (**127**) and (1*S*,6*R*,9*S*,11*R*)-13,14-dihydroxycaryophyll-2(15)-en-7-one (**124**) presented AChE inhibition with IC<sub>50</sub> values of 25.8 and 40.0  $\mu$ M, respectively, the other compounds, pulicaryenne A (**123**), (5*Z*)-14-hydroxycaryophyllen-7-one (**125**), and (1*S*,5*Z*,9*R*)-12-acetoxy-14-hydroxycaryophylla-2(15),5-dien-7-one (**126**) were much weaker as inhibitors of AChE, presenting IC<sub>50</sub> values of 214.9, 108.3, and 101.2  $\mu$ M, respectively. This difference in behavior can be explained by the different substitution pattern on carbons C-5, C-6, and C-11 and the difference in the configuration of the stereogenic centers on the caryophyllene basic scaffold. For instance, when comparing the scaffold of compounds **127** and **124**, the first does not present a C6 asymmetric center being replaced by an endocyclic double bond (C5–C6) [114,124]. The molecule **127** becomes much more planar as the endocyclic bond has the configuration *Z* and is conjugated with the carbonyl group located at C7. When comparing **126** and **127**, the

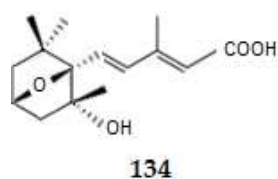
acetylation of the alcohol at C12 on compound **127** explains the attenuation of the AChE inhibition of compound **126** [124].



Artemisinin (**53**), from *A. annua* in Cameroon, exhibits moderate AChE inhibition with an  $IC_{50}$  value of  $103.9 \mu\text{M}$  [125]. Quinanol A (**128**), B (**129**), C (**130**), D (**131**), and E (**132**), and sinenofuranol (**133**), were isolated from *Aquilaria sinensis* (Lour.) Gilg from China. The inhibitory activities against AChE of the isolated sesquiterpenes were evaluated. With a concentration of  $50 \mu\text{g}/\text{mL}$ , compounds **128**–**133** show weak inhibitory activity of AChE with values of 63.1, 15.0, 19.1,  $<10$ ,  $<10$ , and 24.2%, respectively. The compounds **131** and **132** are inactive with inhibition ratios less than 10%. The  $IC_{50}$  value of AChE inhibitory activity of quinanol A (**128**) is  $100.8 \mu\text{M}$  [126].



Megatigma-7,9-diene-1,4-epoxy-2-hydroxy-10-carboxylic acid (**134**), isolated from *Lycopodiastrium casuarinoides* (Spring) Holub (Lycopodiaceae), commonly known as Shu Jin Cao in Chinese, existing in South China, presents anticholinesterase activity inhibiting AChE with an  $IC_{50}$  value of  $9.3 \mu\text{M}$  [127]. The epoxide between C1 and C4 of the cyclohexane confers rigidity to the scaffold of the compound **134** and makes it coplanar with the conjugated system of the compound. These results suggest that the rigidity and planarity of compound **134** makes it a potent inhibitor of AChE.



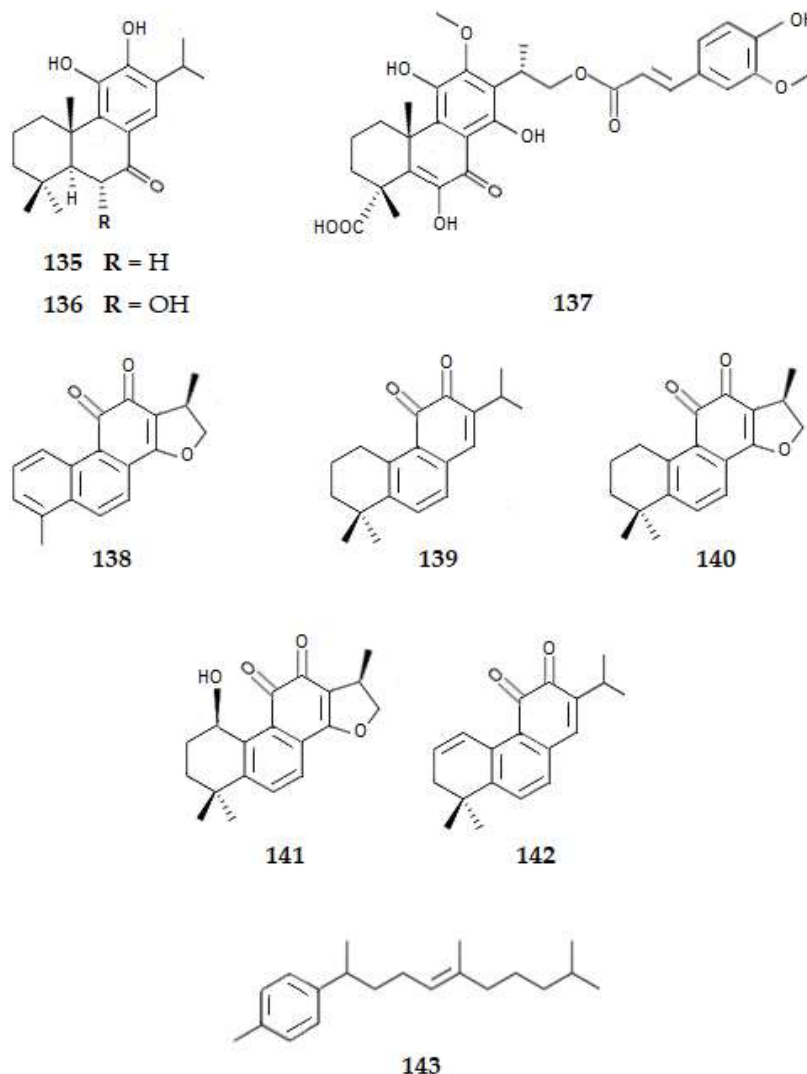
#### 2.4.3. Diterpenes

Several diterpenes isolated from plants have presented high inhibitory activity against AChE.

From *Caryopteris mangolica* Bunge, distributed in Mongolia and Inner Mongolia in China, 12-O-demethylcryptojaponol (**135**) and 6 $\alpha$ -hydroxydemethylcryptojaponol (**136**) inhibited human erythrocyte AChE. The former compound (**135**) inhibits AChE with an IC<sub>50</sub> value of 50.8  $\mu$ M, whereas the latter compound (**136**) is a more active inhibitor of AChE (IC<sub>50</sub> = 19.2  $\mu$ M), suggesting that the presence of the hydroxyl group at the C6 position is important for the inhibition of this cholinesterase [114,128]. Lycocasuarinone A (**137**), another abietane-type diterpene, isolated from *L. casuarinoides*, commonly known as Shu Jin Cao in Chinese, existing in South China, inhibits AChE with an IC<sub>50</sub> value of 26.8  $\mu$ M [127].

Another class of abietane-type diterpenes is constituted by the tanshinones, which can be isolated from the roots of *Salvia* and *Perovskia* species. These compounds have high permeability to cross the BBB. From *Perovskia atriplicifolia* Benth and *Salvia glutinosa* L., 15,16-dihydrotanshinone (**138**) was a very potent inhibitor of AChE with an inhibition of 65.17% at a concentration of 35.8  $\mu$ M. Miltirone (**139**), another tanshinone extracted from the same plants, is inactive as inhibitor of AChE. Cryptotanshinone (**140**), 1 $\beta$ -hydroxycryptotanshinone (**141**), and 1,2-didehydromiltirone (**142**) were also inactive as inhibitors of AChE [129]. These results suggest that the presence of the two aromatic rings and the presence of the furan ring from C15, making 15,16-dihydrotanshinone (**138**) very planar, is responsible for its AChE inhibition.

Pentylcurcumene (**143**), the (6',10'-dimethylundec-5'-en-2' $\alpha$ -yl)-4-methylbenzene, exists in the aerial parts of the leaves of *Geophila repens* (L.) I.M. Johnst of India. Pentylcurcumene (**143**) is a weak inhibitor of AChE exhibiting an IC<sub>50</sub> value of 268.6  $\mu$ M [130].

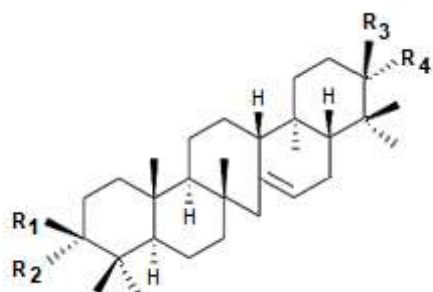


#### 2.4.4. Triterpenes

Three limonoids, extracted from the seeds of *T. welwitschia*, were identified as trichilia lactone D5 (**68**), rohituka 3 (**69**), and dregeanin DM4 (**70**). The  $IC_{50}$  values for the inhibition of AChE were 19.13, 34.15, and 45.69  $\mu$ M, respectively. Thus, compound **70** has a moderate AChE and the others are even weaker inhibitors [114,115].

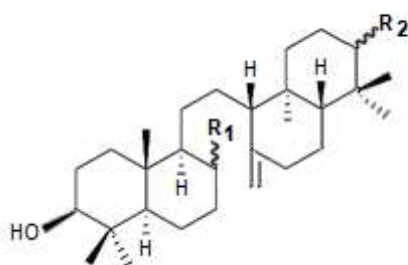
As already mentioned above (Section 2.1.2), twelve serratene-type terpenes (compounds **32–43**) were isolated from *L. cernua*, of Vietnam [76]. While  $3\beta,21\alpha$ -diacetoxyserrat-14 $\beta$ -ol (**37**),  $3\beta,21\beta,29$ -trihydroxyserrat-14-en-3 $\beta$ -yl *p*-dihydrocoumarate (**34**),  $3\beta,14\alpha,15\alpha,21\beta$ -tetrahydroxyserrat-24-oic acid-3 $\beta$ -yl-(40-methoxy-50-hydroxybenzoate) (**33**), and  $21\beta$ -hydroxyserrat-14-en-3,16-dione (**36**) are active as inhibitors of AChE with  $IC_{50}$  values of 0.91, 1.69, 9.98, and 10.67  $\mu$ M, respectively, all the other compounds were inactive ( $IC_{50} > 30 \mu$ M) [114].

Several other serratene-type triterpenes were extracted from *L. casuarinoides*, collected in China, identified as serrat-14-en-3 $\beta,21\alpha$ -diol (**144**), serrat-14-en-3 $\beta,21\beta$ -diol (**145**),  $\alpha$ -onocerin (**146**), 26-nor-8-oxo- $\alpha$ -onocerin (**147**), and 26-nor-8-oxo-21-one- $\alpha$ -onocerin (**148**). While compound **148** exhibits activity as an inhibitor of AChE with an  $IC_{50}$  value of 1.01  $\mu$ M, all the other compounds are inactive ( $IC_{50} > 50 \mu$ M) [127].



**144**  $R_1 = OH; R_2 = H; R_3 = H; R_4 = OH$

**145**  $R_1 = OH; R_2 = H; R_3 = OH; R_4 = H$

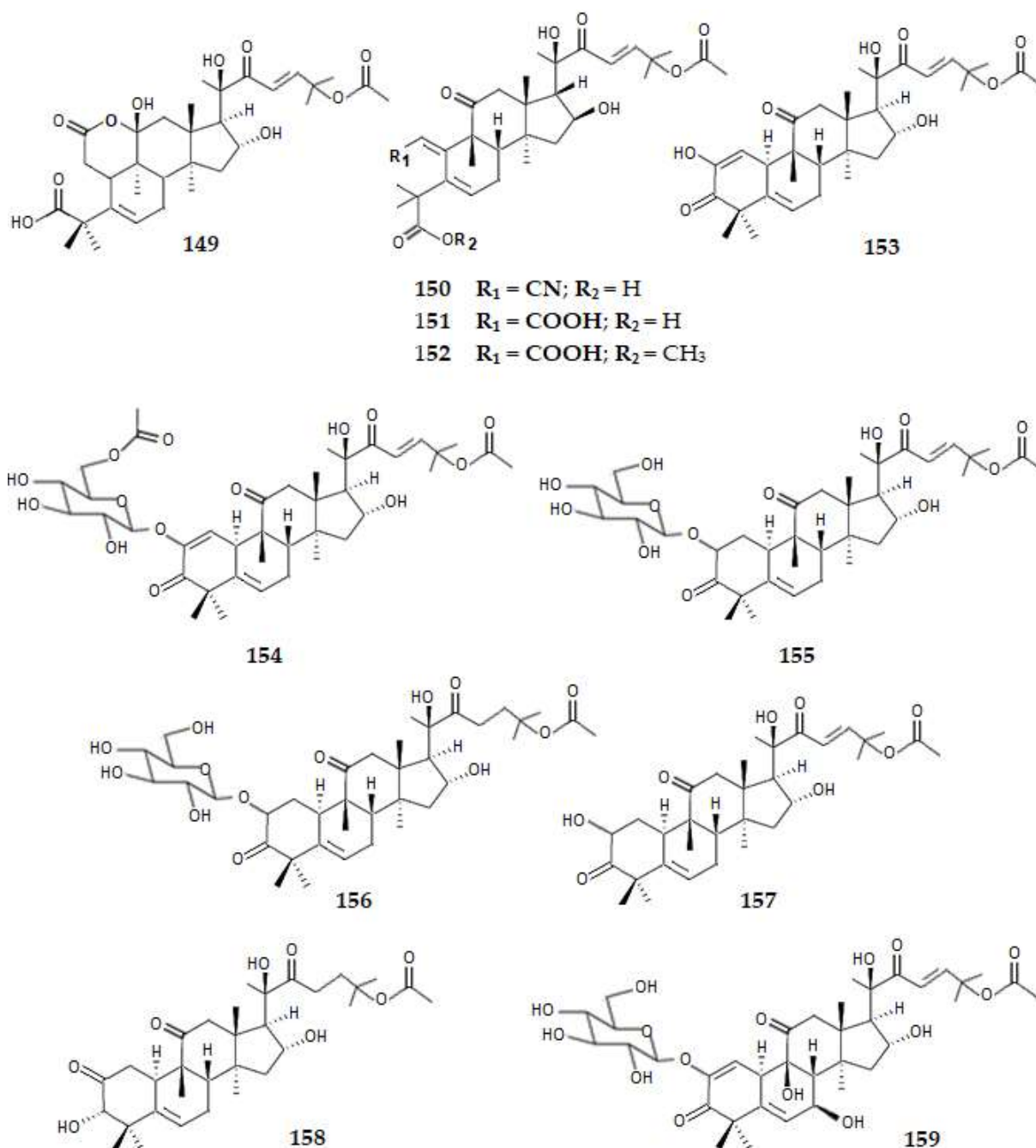


**146**  $R_1 = =CH_2; R_2 = \alpha-OH$

**147**  $R_1 = =O; R_2 = \alpha-OH$

**148**  $R_1 = =O; R_2 = =O$

From the fruits of *Citrullus colocynthis* L. collected at Xinjiang, People's Republic of China, several cucurbitane-type triterpenes were extracted. The compounds were identified as colocynthenin A (**149**), colocynthenin B (**150**), colocynthenin C (**151**), colocynthenin D (**152**), cucurbitacin E (**153**), 6'-acetyl-2-O- $\beta$ -D-glucocucurbitacin E (**154**), arvenin I (**155**), arvenin II (**156**), cucurbitacin B (**157**), 23,24-dihydrocucurbitacin B (**158**), and colocynthoside A (**159**). Colocynthenin A (**149**) and colocynthenin C (**151**) are significant inhibitors of AChE, with  $IC_{50}$  values of 2.6 and 3.1  $\mu$ M, respectively. The other compounds are inactive against AChE ( $IC_{50} > 10 \mu$ M) [114,131].



Forty-three lanostane-type triterpenes (**160–202**) were extracted from the fruiting bodies of *Ganoderma lucidum* (Curtis) Kummer existing in China and Japan [114,132].

Considering the compounds that have conjugated double bonds on the side chain linked to C17 between C24 and C25 and the carboxylic group, such as ganolucidic acid E (**160**), 11 $\beta$ -hydroxy-3,7-dioxo-5 $\alpha$ -lanosta-8,24(*E*)-dien-26-oic acid (**161**), 23*S*-hydroxy-3,7,11,15-tetraoxo-lanost-8,24*E*-diene-26-oic acid (**162**), and ganoderic acid X1 (**163**), the IC<sub>50</sub> values for the AChE inhibition were 13.8, 10.8, >200, and >200  $\mu\text{M}$ , respectively, suggesting that when rings B and C have a conjugated system between them comprising C7, C8, C9, and C11, and a carbonyl group at C15, such as on compounds **162** and **163**, the scaffold is too rigid and planar on that part of the molecule, and thus does not inhibit AChE.

Considering now the compounds that have double bonds on the side chain linked to C17 but are not conjugated with the carboxylic group, like ganoderenic acid D (**164**), ganoderenic acid H (**165**), ganoderic acid K (**166**), 3 $\beta$ ,7 $\beta$ -dihydroxy-11,15,23-trioxo-lanost-8,16-dien-26-oic acid (**167**), ganoderic acid E (**168**), 12-acetoxy-3,7,11,15,23-pentaoxolanost-8,20-

dien-26-oic acid (169), 7 $\beta$ -hydroxy-3,11,15,23-tetraoxo-27 $\xi$ -lanost-8,16-dien-26-oic acid (170), ganoderenic acid B (171), ganoderenic acid F (172), ganoderoid D (173), ganoderoid F (174), ganoderenic acid C (175), and 3 $\beta$ -hydroxyganoderoid D (176), they inhibit AChE with  $IC_{50} > 200 \mu M$ , suggesting the significance for the inhibition of AChE of the conjugated double bonds on the side chain linked to C17 between C24 and C25 and the carboxylic group.

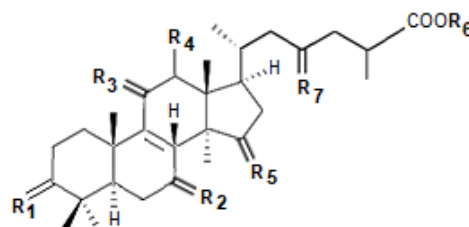
Considering now ganoderic acid H (177), 12 $\beta$ -hydroxyganoderenic acid F (178), methylganoderate F (179), ganoderic acid J (180), ganoderic acid F (181), and ganoderic acid AP (182), all of them are inactive ( $IC_{50} > 200 \mu M$ ) as they have no double bond between carbons on the side chain linked to C17, and rings B and C have a conjugated system between them comprising C7, C8, C9, and C11 and a carbonyl group at C15.

Even compounds having no long conjugated system comprising C7, C8, C9, and C11, but having no double bond between C24 and C25, as is the case for ganolucidic acid E (160) and 11 $\beta$ -hydroxy-3,7-dioxo-5 $\alpha$ -lanosta-8,24(E)-dien-26-oic acid (161), like ganoderic acid B (183), C (184), D (185), G (186), and N (187) and methyl ganoderate G (188), are inactive against AChE ( $IC_{50} > 200 \mu M$ ).

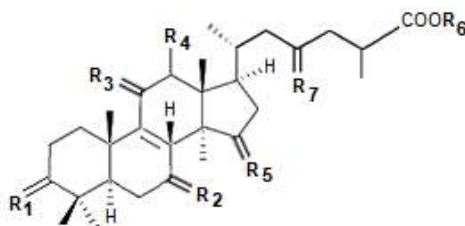
Besides ganolucidic acid E (160) and 11 $\beta$ -hydroxy-3,7-dioxo-5 $\alpha$ -lanosta-8,24(E)-dien-26-oic acid (161), ten other compounds inhibit AChE with  $IC_{50} < 200 \mu M$ . These compounds were identified as ganoderic acid Am1 (189), methyl ganoderate C (190), ganoderoid C1 (191), 12 $\beta$ -hydroxyganoderenic acid F (192), methyl ganoderate E (193), ganoderic acid C6 (194), methyl ganoderic acid C6 (195), ganoderoid A (196), ganoderoid B2 (197), and ganoderolactone G (198) with  $IC_{50}$  values for the inhibition of AChE of 183.0, 148.0, 142.0, 102.0, 45.8, 147.5, 145.2, 149.0, 102.4, and 130.5  $\mu M$ , respectively. All of them are weak inhibitors of AChE. Compared with the significant inhibitory effects presented by ganolucidic acid E (160) and 11 $\beta$ -hydroxy-3,7-dioxo-5 $\alpha$ -lanosta-8,24(E)-dien-26-oic acid (161), it can be concluded that the C17 side chain may serve as the key feature for AChE inhibition, especially when it contains the conjugated double bonds on the side chain linked to C17 between C24 and C25 and the carboxylic group.

Four other compounds, with a different side chain linked to C17, were identified as lucidone A (199), lucidone D (200), ganoderoid B (201), and ganodermanondiol (202). All of them were inactive against AChE ( $IC_{50} > 200 \mu M$ ). These results suggest, again, the significance of the side chain linked to C17.

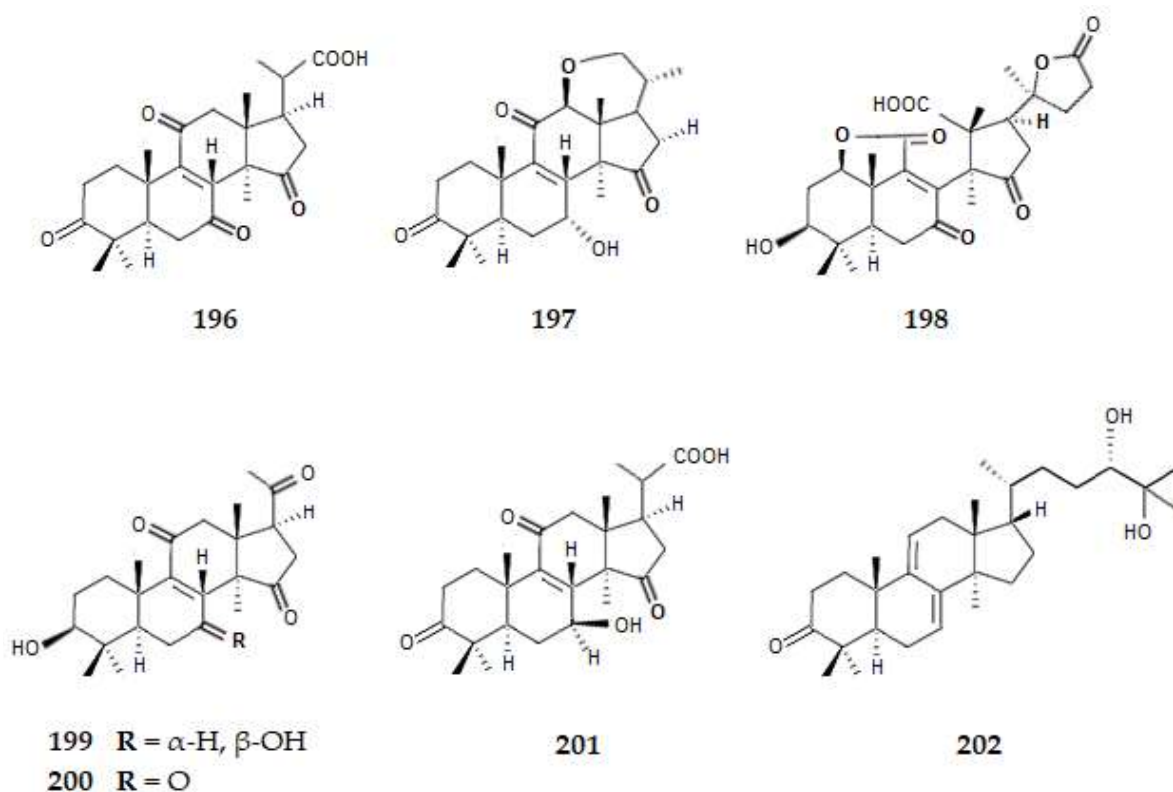
Overall, among the lanostane-type triterpenes extracted from the fruiting bodies of *G. lucidum*, the major components have 30 carbons (known as ganoderic acids), but many of them have 27, 25, or 24 carbons. The results indicate that the C30 ganoderic acids are the main active components for the inhibition of AChE. The structure of the side chain linked to C17 has an important effect on the inhibition of AChE. Indeed, the length of the side chain affects the activity of the lanostane-type triterpenes being ideal, with eight carbons and with a double bond between C24 and C25 and a carboxylic group at C25 [114,132].



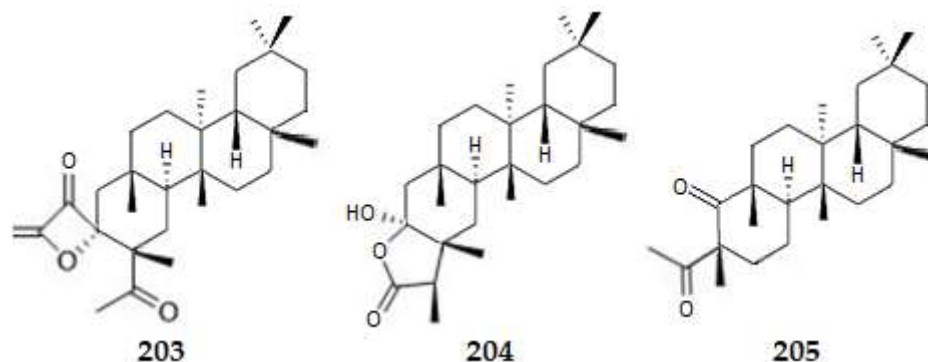
- 160  $\Delta^{24,25}$  R<sub>1</sub> = O; R<sub>2</sub> = H,H; R<sub>3</sub> = O; R<sub>4</sub> = H; R<sub>5</sub> =  $\beta$ -H,  $\alpha$ -OH; R<sub>6</sub> = H; R<sub>7</sub> = H,H  
 161  $\Delta^{24,25}$  R<sub>1</sub> = O; R<sub>2</sub> = O; R<sub>3</sub> =  $\alpha$ -H,  $\alpha$ -OH; R<sub>4</sub> = H; R<sub>5</sub> = H,H; R<sub>6</sub> = H; R<sub>7</sub> = H,H  
 162  $\Delta^{24,25}$  R<sub>1</sub> = O; R<sub>2</sub> = O; R<sub>3</sub> = O; R<sub>4</sub> = H; R<sub>5</sub> = O; R<sub>6</sub> = H; R<sub>7</sub> =  $\alpha$ -H,  $\beta$ -OH  
 163  $\Delta^{24,25}$ , 20-OH R<sub>1</sub> = O; R<sub>2</sub> = O; R<sub>3</sub> = O; R<sub>4</sub> =  $\beta$ -OAc; R<sub>5</sub> = O; R<sub>6</sub> = H; R<sub>7</sub> = H,H



- 164  $\Delta^{20,22}$   $R_1 = O$ ;  $R_2 = \alpha\text{-H}, \beta\text{-OH}$ ;  $R_3 = O$ ;  $R_4 = H$ ;  $R_5 = O$ ;  $R_6 = H$ ;  $R_7 = O$
- 165  $\Delta^{20,22}$   $R_1 = \alpha\text{-H}, \beta\text{-OH}$ ;  $R_2 = O$ ;  $R_3 = O$ ;  $R_4 = H$ ;  $R_5 = O$ ;  $R_6 = H$ ;  $R_7 = O$
- 166  $\Delta^{20,22}$   $R_1 = \alpha\text{-H}, \beta\text{-OH}$ ;  $R_2 = \alpha\text{-H}, \beta\text{-OH}$ ;  $R_3 = O$ ;  $R_4 = \beta\text{-OAc}$ ;  $R_5 = O$ ;  $R_6 = H$ ;  $R_7 = O$
- 167  $\Delta^{16,17}$   $R_1 = \alpha\text{-H}, \beta\text{-OH}$ ;  $R_2 = \alpha\text{-H}, \beta\text{-OH}$ ;  $R_3 = O$ ;  $R_4 = H$ ;  $R_5 = O$ ;  $R_6 = H$ ;  $R_7 = O$
- 168  $\Delta^{20,22}$   $R_1 = O$ ;  $R_2 = \alpha\text{-H}, \beta\text{-OH}$ ;  $R_3 = O$ ;  $R_4 = \beta\text{-OH}$ ;  $R_5 = O$ ;  $R_6 = H$ ;  $R_7 = O$
- 169  $\Delta^{20,22}$   $R_1 = O$ ;  $R_2 = O$ ;  $R_3 = O$ ;  $R_4 = \beta\text{-OAc}$ ;  $R_5 = O$ ;  $R_6 = H$ ;  $R_7 = O$
- 170  $\Delta^{16,17}$   $R_1 = O$ ;  $R_2 = \alpha\text{-H}, \beta\text{-OH}$ ;  $R_3 = O$ ;  $R_4 = H$ ;  $R_5 = O$ ;  $R_6 = H$ ;  $R_7 = O$
- 171  $\Delta^{20,22}$   $R_1 = \alpha\text{-H}, \beta\text{-OH}$ ;  $R_2 = \alpha\text{-H}, \beta\text{-OH}$ ;  $R_3 = O$ ;  $R_4 = H$ ;  $R_5 = O$ ;  $R_6 = H$ ;  $R_7 = O$
- 172  $\Delta^{20,22}$   $R_1 = O$ ;  $R_2 = O$ ;  $R_3 = O$ ;  $R_4 = H$ ;  $R_5 = O$ ;  $R_6 = H$ ;  $R_7 = O$
- 173  $\Delta^{17,20}$   $R_1 = O$ ;  $R_2 = O$ ;  $R_3 = O$ ;  $R_4 = \beta\text{-OAc}$ ;  $R_5 = O$ ;  $R_6 = H$ ;  $R_7 = O$
- 174  $\Delta^{20,22}$   $R_1 = \alpha\text{-H}, \beta\text{-OH}$ ;  $R_2 = \alpha\text{-H}, \beta\text{-OH}$ ;  $R_3 = O$ ;  $R_4 = \alpha\text{-OH}$ ;  $R_5 = O$ ;  $R_6 = \text{CH}_3$ ;  $R_7 = O$
- 175  $\Delta^{20,22}$   $R_1 = \alpha\text{-H}, \beta\text{-OH}$ ;  $R_2 = \alpha\text{-H}, \beta\text{-OH}$ ;  $R_3 = O$ ;  $R_4 = H$ ;  $R_5 = \beta\text{-H}, \alpha\text{-OH}$ ;  $R_6 = H$ ;  $R_7 = O$
- 176  $\Delta^{17,20}$   $R_1 = \alpha\text{-H}, \beta\text{-OH}$ ;  $R_2 = O$ ;  $R_3 = O$ ;  $R_4 = \beta\text{-OAc}$ ;  $R_5 = O$ ;  $R_6 = H$ ;  $R_7 = O$
- 177  $R_1 = \alpha\text{-H}, \beta\text{-OH}$ ;  $R_2 = O$ ;  $R_3 = O$ ;  $R_4 = \beta\text{-OAc}$ ;  $R_5 = O$ ;  $R_6 = H$ ;  $R_7 = O$
- 178  $R_1 = O$ ;  $R_2 = O$ ;  $R_3 = O$ ;  $R_4 = \beta\text{-OH}$ ;  $R_5 = O$ ;  $R_6 = H$ ;  $R_7 = O$
- 179  $R_1 = O$ ;  $R_2 = O$ ;  $R_3 = O$ ;  $R_4 = \beta\text{-OAc}$ ;  $R_5 = O$ ;  $R_6 = \text{CH}_3$ ;  $R_7 = O$
- 180  $R_1 = O$ ;  $R_2 = O$ ;  $R_3 = O$ ;  $R_4 = H$ ;  $R_5 = \beta\text{-H}, \alpha\text{-OH}$ ;  $R_6 = H$ ;  $R_7 = O$
- 181  $R_1 = O$ ;  $R_2 = O$ ;  $R_3 = O$ ;  $R_4 = \beta\text{-OAc}$ ;  $R_5 = O$ ;  $R_6 = H$ ;  $R_7 = O$
- 182 20-OH  $R_1 = O$ ;  $R_2 = O$ ;  $R_3 = O$ ;  $R_4 = \beta\text{-OAc}$ ;  $R_5 = O$ ;  $R_6 = H$ ;  $R_7 = O$
- 183  $R_1 = \alpha\text{-H}, \beta\text{-OH}$ ;  $R_2 = \alpha\text{-H}, \beta\text{-OH}$ ;  $R_3 = O$ ;  $R_4 = H$ ;  $R_5 = O$ ;  $R_6 = H$ ;  $R_7 = O$
- 184  $R_1 = O$ ;  $R_2 = \alpha\text{-H}, \beta\text{-OH}$ ;  $R_3 = O$ ;  $R_4 = H$ ;  $R_5 = O$ ;  $R_6 = H$ ;  $R_7 = O$
- 185  $R_1 = O$ ;  $R_2 = \alpha\text{-H}, \beta\text{-OH}$ ;  $R_3 = O$ ;  $R_4 = \beta\text{-OH}$ ;  $R_5 = O$ ;  $R_6 = H$ ;  $R_7 = O$
- 186  $R_1 = \alpha\text{-H}, \beta\text{-OH}$ ;  $R_2 = \alpha\text{-H}, \beta\text{-OH}$ ;  $R_3 = O$ ;  $R_4 = \beta\text{-OH}$ ;  $R_5 = O$ ;  $R_6 = H$ ;  $R_7 = O$
- 187 20-OH  $R_1 = O$ ;  $R_2 = \alpha\text{-H}, \beta\text{-OH}$ ;  $R_3 = O$ ;  $R_4 = H$ ;  $R_5 = O$ ;  $R_6 = H$ ;  $R_7 = O$
- 188  $R_1 = \alpha\text{-H}, \beta\text{-OH}$ ;  $R_2 = \alpha\text{-H}, \beta\text{-OH}$ ;  $R_3 = O$ ;  $R_4 = \alpha\text{-OH}$ ;  $R_5 = O$ ;  $R_6 = \text{CH}_3$ ;  $R_7 = O$
- 189  $R_1 = \alpha\text{-H}, \beta\text{-OH}$ ;  $R_2 = O$ ;  $R_3 = O$ ;  $R_4 = H$ ;  $R_5 = O$ ;  $R_6 = H$ ;  $R_7 = O$
- 190  $R_1 = O$ ;  $R_2 = \alpha\text{-H}, \beta\text{-OH}$ ;  $R_3 = O$ ;  $R_4 = H$ ;  $R_5 = O$ ;  $R_6 = \text{CH}_3$ ;  $R_7 = O$
- 191  $R_1 = \alpha\text{-H}, \beta\text{-OH}$ ;  $R_2 = O$ ;  $R_3 = O$ ;  $R_4 = \beta\text{-OH}$ ;  $R_5 = O$ ;  $R_6 = H$ ;  $R_7 = O$
- 192  $\Delta^{20,22}$   $R_1 = O$ ;  $R_2 = O$ ;  $R_3 = O$ ;  $R_4 = \beta\text{-OH}$ ;  $R_5 = O$ ;  $R_6 = H$ ;  $R_7 = O$
- 193  $R_1 = O$ ;  $R_2 = O$ ;  $R_3 = O$ ;  $R_4 = H$ ;  $R_5 = O$ ;  $R_6 = \text{CH}_3$ ;  $R_7 = O$
- 194  $R_1 = \alpha\text{-H}, \beta\text{-OH}$ ;  $R_2 = O$ ;  $R_3 = O$ ;  $R_4 = \beta\text{-OH}$ ;  $R_5 = O$ ;  $R_6 = H$ ;  $R_7 = O$
- 195  $R_1 = \alpha\text{-H}, \beta\text{-OH}$ ;  $R_2 = H, H$ ;  $R_3 = O$ ;  $R_4 = \beta\text{-OH}$ ;  $R_5 = O$ ;  $R_6 = \text{CH}_3$ ;  $R_7 = O$

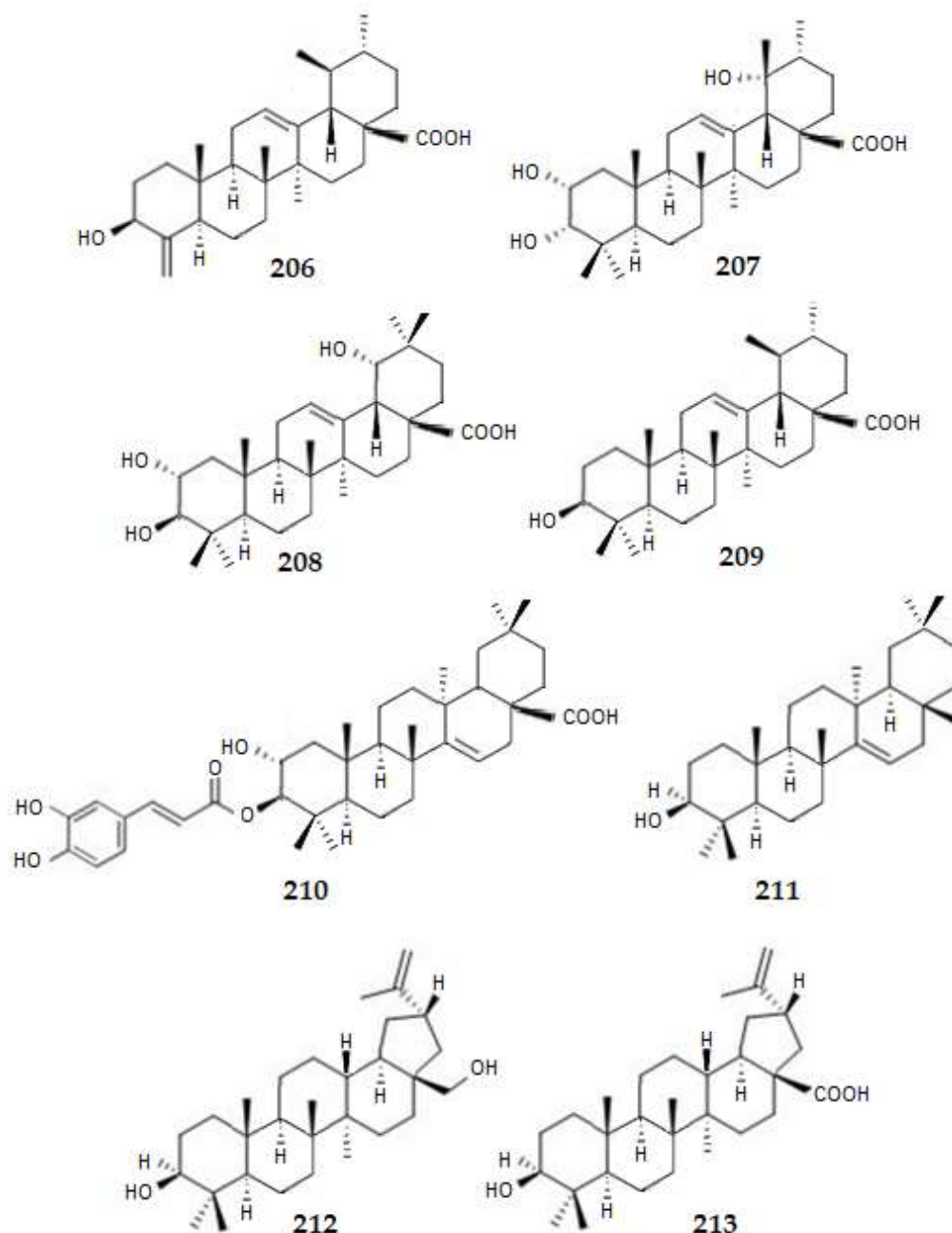


From the branches and roots of *Malpighia emarginata* DC, cultivated in China, three friedelanes, pentacyclic triterpenes, were isolated, namely, norfriedelins A (**203**), B (**204**), and C (**205**). They presented AChE inhibition with  $IC_{50}$  values of 10.3, 28.7, and  $>50$   $\mu$ M, respectively. The higher activity against AChE of norfriedelin A (**203**) when compared to norfriedelin B (**204**) might be due to the presence of the  $\alpha$ -oxo- $\beta$ -lactone group on compound **203** instead of the lactone group on the compound **204** [114,133].



$3\beta$ -Hydroxy-24-nor-urs-4(23)-12-dien-28-oic acid (**206**) was isolated from *Patrinia scabiosaefolia* Siebold & Zucc., from China. Compound **206** exhibits activity against AChE with an  $IC_{50}$  value of 10.0  $\mu$ M [113,114]. Three other moderate inhibitors of AChE were extracted from the leaves of *Callicarpa maingayi* K & G in Malaysia, namely, euscaphic acid (**207**), arjunic acid (**208**), and ursolic acid (**209**). These compounds inhibit AChE with  $IC_{50}$  values of 35.9, 37.5, and 21.5  $\mu$ M, respectively. These results demonstrate that ursolic acid (**209**), with only one hydroxyl group at C3, has more potent AChE inhibition than euscaphic acid (**207**) and arjunic acid (**208**), which have three hydroxyl groups at C2, C3, and C19 [114,134]. This suggests that the two other hydroxyl groups (at C2 and C19) will prevent the molecule from docking into the active pocket of AChE by hydrogen bonding. Other triterpenes were isolated from the bark of *Garcinia hombroniana* Pierre, in Malaysia. They were identified as 2-hydroxy-3 $\alpha$ -O-caffeoyltaraxar-14-en-28-oic acid (**210**), taraxerol (**211**), betulin (**212**), and betulinic acid (**213**). Compound **210** is the most potent

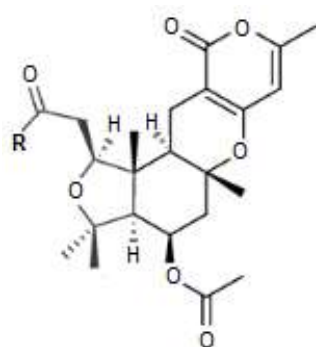
inhibitor of AChE exhibiting an  $IC_{50}$  value of 13.5  $\mu$ M, while compounds **212** and **213** exhibit  $IC_{50}$  values of 28.5 and 24.2  $\mu$ M, respectively. The  $IC_{50}$  value for compound **211** was not determined. Molecular docking analysis showed that 2-hydroxy-3-O-caffeoyltaraxar-14-en-28-oic acid (**210**) interacts with the catalytic and peripheral binding sites of AChE by forming three hydrogen bonds, one with the amino acid Tyr 334, one with His 440, and the last with Ser 200 [114,135].



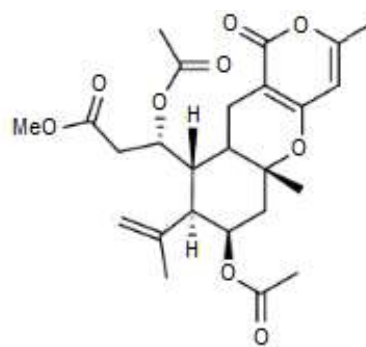
#### 2.4.5. Meroterpenes

The inhibition of AChE by several meroterpenes, extracted from the fungus *Aspergillus versicolor* (Vuill.) Tirab. obtained from the mud of the South China Sea, was evaluated. Asperversins A (**214**), B (**215**), C (**216**), D (**217**), E (**218**), and F (**219**), and the related compound asperdemin (**220**), are inactive ( $IC_{50} > 40 \mu$ M). Asperversin G (**221**) exhibits AChE inhibition with an  $IC_{50}$  value of 13.6  $\mu$ M. Molecular docking studies were conducted for asperversin G (**221**) to obtain an insight into the binding pattern of the binding of the compound with AChE. The basic skeleton of compound **221** provides a better binding than

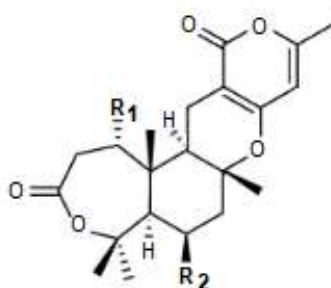
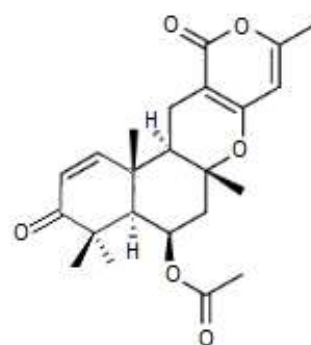
the other asperversins, forming several hydrogen bonding interactions with the amino acid residues Glu 291 and Tyr 341. These results suggest that the  $\alpha$ ,  $\beta$ -unsaturated ketone group is important for the inhibition of AChE [136].

214 R = OCH<sub>3</sub>

215 R = O



216

217 R<sub>1</sub> = OH; R<sub>2</sub> = H218 R<sub>1</sub> = OH; R<sub>2</sub> = OAc219 R<sub>1</sub> = OAc; R<sub>2</sub> = OH220 R<sub>1</sub> = OH; R<sub>2</sub> = OH

221

### 3. Discussion

At present, 221 terpenes, isolated mainly from plants, have been studied as possible anti-AD agents: 2 (0.9%) tetraterpenes, 114 (51.6%) triterpenes, 17 (7.7%) diterpenes, 35 (15.8%) sesquiterpenes, 24 (10.9%) monoterpenes, and 29 (13.1%) meroterpenes.

The most active terpenes against BACE1 are the meroterpenes asperterpene B (**12**) (IC<sub>50</sub> = 0.06  $\mu$ M) and asperterpene A (**11**) (IC<sub>50</sub> = 0.08  $\mu$ M), followed by the triterpene 21 $\beta$ -hydroxyserrat-14-en-3,16-dione (**36**) (IC<sub>50</sub> = 0.2  $\mu$ M). These results suggest that in asperterpene A (**11**) and B (**12**), the 1,2,5-trimethyl-4,9-dioxobicyclo[3.3.1]non-2-ene-3-carboxylic acid moiety is significant for the inhibition of BACE1. Indeed, the bridge between carbons C1 and C4 of the cyclooctene and the extended conjugated system comprising the double bond between C2 and C3, the carboxylic group linked to C3, and the carbonyl group of C4 makes the molecule planar. Concerning the triterpenes, the conjugated system comprising the double bond between C14 and C15 and the carbonyl group of C16 of 21 $\beta$ -hydroxyserrat-14-en-3,16-dione (**36**) makes the ring more planar. Thus, planarity and an extensive  $\pi$  system in the molecule is one of the requirements for terpenes be active against BACE1.

Tetrahydroaplysulphurin-1 (**5**), a gracilin, increases the levels of the inactive isoform of GSK3 $\beta$  (57.1  $\pm$  24.75%) at 0.1  $\mu$ M. All the other gracilins (compounds **3**, **4**, and **6**) are inactive, suggesting that the fusion of the three rings on the scaffold of tetrahydroaplysulphurin-1 (**5**) is significant for the inhibition of GSK3 $\beta$ . Unfortunately, this is the only result for the

inhibition of GSK3 $\beta$ , thus not allowing any other structure–inhibition relationships of GSK3 $\beta$  for the terpene compounds.

The triterpenes methyl kulonate (methyl 3-oxo-16 $\beta$ -hydroxyeuropa-7,24-dien-21-oate) (**66**) and 3 $\beta$ -hydroxy-24-nor-urs-4(23),12-dien-28-oic acid (**67**) exhibit potent inhibitory activity against NO production, with IC<sub>50</sub> values of 4.6 and 10.1  $\mu$ M, respectively. Compound **66** presents on its scaffold a carbonyl group at C3, rendering planarity to ring A, as well as possible  $\pi$ - $\pi$  stacking interactions with the enzyme. The double bond between C7 and C8 renders planarity to rings B and C. Compound **67** presents on its scaffold an exocyclic double bond between C4 and C23, also rendering planarity to ring A, as well as possible  $\pi$ - $\pi$  stacking interactions with the enzyme. The double bond between C12 and C13 renders planarity to rings C and D.

When considering the terpenes that inhibit AChE, the serratene-type terpene 3 $\beta$ ,21 $\alpha$ -diacetoxyserrat-14 $\beta$ -ol (**37**) is the most active terpene as inhibitor of AChE (IC<sub>50</sub> = 0.9  $\mu$ M). Comparing the scaffold of 3 $\beta$ ,21 $\alpha$ -diacetoxyserrat-14 $\beta$ -ol (**37**) with that presented by 3 $\beta$ ,21 $\beta$ ,29-trihydroxyserrat-14-en-3 $\beta$ -yl *p*-dihydrocoumarate (**34**) (IC<sub>50</sub> = 1.7  $\mu$ M), it can be concluded that the presence of an acetyl group on C21 (compound **37**) increases the activity when it replaces a hydroxy group (compound **34**). 26-Nor-8-oxo-21-one- $\alpha$ -onocerin (**148**) (IC<sub>50</sub> = 1.0  $\mu$ M) also presents two carbonyl groups but in different carbons (C8 and C21). In conclusion, the presence of the two carbonyl groups is significant for the inhibition of AChE when serratene-type terpenes are considered.

The cucurbitane-type triterpenes colocynthenin A (**149**) (IC<sub>50</sub> = 2.6  $\mu$ M) and colocynthenin C (**151**) (IC<sub>50</sub> = 3.1  $\mu$ M) are significant inhibitors of AChE, suggesting that the opening of ring A of the triterpene and the presence of a carboxylic group is significant for the inhibition of AChE for the scaffold of cucurbitane-type triterpenes.

The sesquiterpene megatigma-7,9-diene-1,4-epoxy-2-hydroxy-10-carboxylic acid (**134**) also presents an important inhibition of AChE (IC<sub>50</sub> = 9.3  $\mu$ M). The epoxide between C1 and C4 of the cyclohexane confers rigidity to the scaffold of the compound **134** and makes it coplanar with the conjugated system of the compound. These results suggest that the rigidity and planarity of compound **134** makes it a potent inhibitor of AChE.

Comparing forty-three lanostane-type triterpenes, ganolucidic acid E (**160**) (IC<sub>50</sub> = 13.8  $\mu$ M) and 1 $\beta$ -hydroxy-3,7-dioxo-5 $\alpha$ -lanosta-8,24(*E*)-dien-26-oic acid (**161**) (IC<sub>50</sub> = 10.8  $\mu$ M) were the most potent inhibitors of AChE. These results suggest that the scaffold of these lanostane-type triterpenes should contain conjugated double bonds on the side chain linked to C17 between C24 and C25 and the carboxylic group. The results also suggest that these compounds should have two double bonds between rings B and C, but not an extended conjugated system between them comprising C7, C8, C9, and C11 and a carbonyl group at C15, as the scaffold is too rigid and planar on that part of the molecule. These results were supported by molecular docking studies for ganolucidic acid E (**160**), where the hydroxyl group of C15 and the carboxylic group of C25 interact with Leu-138 and Val-132 by hydrogen bonding, respectively. For 11 $\beta$ -hydroxy-3,7-dioxo-5 $\alpha$ -lanosta-8,24(*E*)-dien-26-oic acid (**161**), hydrogen bonds are formed between the hydroxyl group of C11 and the carboxylic group of C25, which interact with Val-132 [114,132]. For the active pocket, the docking analysis suggests that compounds **160** and **161** could dock into the pocket with whole molecules, explaining why the scaffold for rings B and C cannot be too rigid or planar.

Norfriedelins are other triterpene compounds presenting activity as AChE inhibitors. Norfriedelin A (**203**) (IC<sub>50</sub> = 10.3  $\mu$ M) presented the highest activity against AChE, suggesting that the presence of the  $\alpha$ -oxo- $\beta$ -lactone group is important for that inhibition [114,133].

3 $\beta$ -Hydroxy-24-nor-urs-4(23)-12-dien-28-oic acid (**206**) (IC<sub>50</sub> = 10.0  $\mu$ M) exhibits the highest activity when several triterpenes with a similar scaffold are compared. These results demonstrate that these compounds should have only one hydroxyl group at C3. The presence of other hydroxyl groups will prevent the molecule from docking into the active pocket of AChE by hydrogen bonding.

Asperversin G (221) exhibits an  $IC_{50}$  value of 13.6  $\mu$ M, suggesting that the  $\alpha,\beta$ -unsaturated ketone group is important for the inhibition of AChE [136].

#### 4. Conclusions

The results reported in this review only concern the inhibition of one enzyme each time, considering the interaction of one terpene with the active site of that enzyme. Nevertheless, AD is a complex disease due to its multi-factorial origin, involving several mechanisms which may work altogether through interaction between genetic, molecular, and cellular events. Thus, using a polypharmacological approach, concerning the interactions with the active sites of several enzymes, can be highly advantageous as compared to single-target drugs. The polypharmacological therapy can be achieved using either combinations of multiple drugs or multi-target drug ligands (MTDLs) [16,53,137–140]. However, according to the literature [141], a successful strategy to combat AD might be the use of the latter approach. In fact, in the MTDL therapy, where only one active molecule is administered, there is no risk of drug–drug interactions as in the case of a combination therapy or drug cocktail, where each drug has an active component for the inhibition of one of the mechanisms of AD. Additionally, the prevision of pharmacokinetic and pharmacodynamic properties is simplified as there is only one single compound modulating multiple targets simultaneously [141].

Analyzing the scaffold of the selected terpenes, which inhibit one of the mechanisms of AD clinical indications, it is concluded that it is impossible to obtain a molecule which be active against the several enzymes considered. Indeed, each enzyme is very stereoselective and it is not possible to obtain a molecule with the configuration needed to interact with all the enzymes. The selected molecules are all different and, by linking all of them, the result will be a molecule with many carbons, which will not obey Lipinski's rule of five. Thus, using a drug cocktail of aspertene B (12), tetrahydroaplysulphurin-1 (5), methyl kulonate (66), and 3 $\beta$ ,21 $\alpha$ -diacetoxyserratane-14 $\beta$ -ol (37) might be more advantageous.

**Author Contributions:** Conceptualization, J.M. and E.L.; writing, J.M. and E.L. All authors have read and agreed to the published version of the manuscript.

**Funding:** This research received no external funding.

**Institutional Review Board Statement:** Not applicable.

**Informed Consent Statement:** Not applicable.

**Data Availability Statement:** Not applicable.

**Conflicts of Interest:** The authors declare no conflicts of interest.

## Appendix A

Table A1. Terpenes from natural sources with neurological activities and their mode of action.

N.	Terpene (T)				Inhibition (I)		
	Name	Class	Source	Log $P^1$	Mechanism	IC <sub>50</sub> (μM) or I (%)	Refs.
1	Linalool	MonoT	Plant	2.97	BACE1 P-IF (NO) AChE	IN ND IN	[63] [78,79] [121]
2	2,3,4,4-Tetramethyl-5-methylene-cyclopent-2-enone	MonoT	Plant	1.7	BACE1	31.8% at 45 μM	[63]
3	Gracilin L	DiT	Sponge	ND	BACE1	24.6% at 1 μM	[64,65]
4	Gracilin H	DiT	Sponge	3.1	BACE1 P-IF	<24% at 1 μM ND	[64,65] [101]
5	Tetrahydroaplysulphurin-1	DiT	Sponge	4.6	BACE1 GSK3β P-IF	<24% at 1 μM 57.1% at 1 μM ND	[64,65] [65] [101]
6	Gracilin A	DiT	Sponge	5.1	BACE1 P-IF	IN ND	[64,65] [101]
7	Ginsenoside Rg1	TriT	Plant	2.7	BACE1	6.2	[64,66]
8	Ginsenoside Re	TriT	Plant	ND	BACE1	ND	[64,67]
9	Ginsenoside Rg3	TriT	Plant	4.0	BACE1 P-IF	ND ND	[64,68] [102–104]
10	Pseudoginsenoside-F11	TriT	Plant	1.9	BACE1	ND	[69,70]
11	Asperterpene A	MeroT	Fungus	ND	BACE1	0.08	[73,74]
12	Asperterpene B	MeroT	Fungus	ND	BACE1	0.06	[73,74]
13	Asperterpene E	MeroT	Fungus	2.0	BACE1	3.3	[73,74]
14	Asperterpene F	MeroT	Fungus	2.1	BACE1	5.9	[73,74]
15	Asperterpene J	MeroT	Fungus	1.5	BACE1	31.7	[73,74]
16	Asperterpene D	MeroT	Fungus	1.0	BACE1	>50.0	[73,74]
17	Asperterpene G	MeroT	Fungus	2.0	BACE1	>50.0	[73,74]
18	Asperterpene H	MeroT	Fungus	2.4	BACE1	>50.0	[73,74]
19	Asperterpene I	MeroT	Fungus	1.8	BACE1	>50.0	[73,74]
20	Asperterpene K	MeroT	Fungus	2.1	BACE1	>50.0	[73,74]
21	Asperterpene L	MeroT	Fungus	1.7	BACE1	>50.0	[73,74]
22	Asperterpene M	MeroT	Fungus	2.6	BACE1	>50.0	[73,74]
23	Terretonin	MeroT	Fungus	1.2	BACE1	>50.0	[74]
24	Terretonin A	MeroT	Fungus	2.2	BACE1	>50.0	[74]
25	Terretonin D	MeroT	Fungus	2.0	BACE1	>50.0	[74]
26	Terretonin G	MeroT	Fungus	1.5	BACE1	>50.0	[74]

Table A1. Cont.

N.	Terpene (T)				Inhibition (I)		
	Name	Class	Source	Log P <sup>1</sup>	Mechanism	IC <sub>50</sub> (μM) or I (%)	Refs.
27	Terretonin H	MeroT	Fungus	1.9	BACE1	>50.0	[74]
28	Terreusterpene A	MeroT	Fungus	1.8	BACE1	6.0	[75]
29	Terreusterpene B	MeroT	Fungus	2.5	BACE1	11.4	[75]
30	Terreusterpene C	MeroT	Fungus	1.5	BACE1	>40.0	[75]
31	Terreusterpene D	MeroT	Fungus	1.2	BACE1	1.9	[75]
32	3β,21β,29-Trihydroxyserrat-14-en-24-oic acid-3b-yl-(70-hydroxycinnamate)	TriT	Plant	ND	BACE1	1.1	[76]
33	3β,14α,15α,21β-Tetrahydroxyserrat-24-oic acid-3β-yl-(40-methoxy-50-hydroxybenzoate)	TriT	Plant	ND	BACE1	>30.0	[76,114]
					AChE	1.0	[76]
34	3β,21β,29-Trihydroxyserrat-14-en-3β-yl <i>p</i> -dihydrocoumarate	TriT	Plant	ND	BACE1	10.0	[76,114]
					AChE	>10.0	[76]
35	3β,21β,29-Trihydroxyserrat-14-en-24-oic acid-3β-yl-(40-hydroxybenzoate)	TriT	Plant	ND	BACE1	1.7	[76,114]
					AChE	0.3	[76]
36	21β-Hydroxyserrat-14-en-3,16-dione	TriT	Plant	ND	BACE1	>30	[76,114]
					AChE	0.2	[76]
37	3β,21α-Diacetoxyserrat-14β-ol	TriT	Plant	ND	BACE1	10.7	[76,114]
					AChE	>10	[76]
38	Serrat-14-en-3α,21α-diol	TriT	Plant	ND	BACE1	0.9	[76,114]
					AChE	>10.0	[76]
39	3β,21β,29-Trihydroxy-16-oxoserrat-14-en-24-oic acid	TriT	Plant	ND	BACE1	>30.0	[76,114]
					AChE	>10.0	[76]
40	Serrat-14-en-3α,21β-diol	TriT	Plant	ND	BACE1	>30.0	[76,114]
					AChE	>10.0	[76]
41	3β,21β,29-Trihydroxy-16-oxoserrat-14-en-24-methyl ester	TriT	Plant	ND	BACE1	>30.0	[76,114]
					AChE	>10.0	[76]
42	3β,21α-Dihydroxyserrat-14β-ol	TriT	Plant	ND	BACE1	>30.0	[76,114]
					AChE	>10.0	[76]
43	3α,21β-Dihydroxy-16-oxoserrat-14-en-24-oic acid	TriT	Plant	ND	BACE1	>30.0	[76,114]
					AChE	>10.0	[76]
44	(+)-Limonene	MonoT	Plant	3.4	P-IF	ND	[77]
45	Thymoquinone	MonoT	Plant	2.0	P-IF	ND	[80–82]
46	Carvacrol	MonoT	Plant	3.1	P-IF	ND	[83]
47	1,8-Cineol	MonoT	Plant	2.5	P-IF	ND	[78,84]
					AChE	IN	[121]
48	α-Pinene	MonoT	Plant	2.8	P-IF	ND	[78,84]
					AChE	IN	[121]
49	<i>p</i> -Cymene	MonoT	Plant	4.1	P-IF	ND	[78,85]
					AChE	IN	[121]
50	Carvacryl acetate	MonoT	Plant	3.0	P-IF	ND	[78,86–88]

Table A1. Cont.

N.	Terpene (T)				Inhibition (I)		
	Name	Class	Source	Log P <sup>1</sup>	Mechanism	IC <sub>50</sub> (μM) or I (%)	Refs.
51	Borneol	MonoT	Plant	2.7	P-IF	ND	[78,86–88]
52	Geraniol	MonoT	Plant	2.9	P-IF	ND	[78,86–88]
53	Artemisinin	SesquiT	Plant	2.8	P-IF AChE	ND 103.9	[89] [125]
54	Parthenolide	SesquiT	Plant	2.3	P-IF	ND	[91–93]
55	7β-(3-Ethyl-cis-crotonoyloxy)-1α-(2-methylbutyryloxy)-3,14-dehy-dro-Z-notonipetranone (ECN)	SesquiT	Plant	ND	P-IF	ND	[78,91]
56	α-Cyperone	SesquiT	Plant	3.8	P-IF	ND	[78,92–94]
57	Lactucopicrin	SesquiT	Plant	1.1	P-IF	ND	[78,92–94]
58	Bakkenolide B	SesquiT	Plant	3.3	P-IF	ND	[78,92–94]
59	Carnosic acid	DiT	Plant	4.9	P-IF	ND	[89,95,96]
60	Ginkgolide A	DiT	Plant	0.6	P-IF	ND	[97–100]
61	Ginkgolide B	DiT	Plant	0.4	P-IF	ND	[97–100]
62	Ginkgolide C	DiT	Plant	1.4	P-IF	ND	[97–100]
63	Ginsenoside Rd	TriT	Plant	2.4	P-IF	ND	[78,108,109]
64	Protopanaxatriol (PPT)	TriT	Plant	5.9	P-IF	ND	[78,108,109]
65	Gypenoside XVII	TriT	Plant	1.9	P-IF	ND	[78,111]
66	Methyl kulonate	TriT	Plant	6.4	P-IF (NO)	4.6	[112]
67	3β-Hydroxy-24-nor-urs-4(23),12-dien-28-oic acid	TriT	Plant	ND	P-IF (NO)	10.1	[113]
68	Trichilia lactone D5	TriT	Plant	ND	P-IF (NO) AChE	>4.0 19.1	[114,115] [114,115]
69	Rohituka 3	TriT	Plant	1.8	P-IF (NO) AChE	3.0 34.2	[114,115] [114,115]
70	Dregeanin DM4	TriT	Plant	2.6	P-IF (NO) AChE	2.9 45.7	[114,115] [114,115]
71	2-Hydroxyxylorumpihiin F	TriT	Plant	3.9	P-IF (NO)	24.5	[116]
72	Xylorumpihiin E	TriT	Plant	3.9	P-IF (NO)	>50.0	[116]
73	Xylorumpihiin F	TriT	Plant	ND	P-IF (NO)	>50.0	[116]
74	Xylorumpihiin G	TriT	Plant	3.9	P-IF (NO)	>50.0	[116]
75	Xylorumpihiin H	TriT	Plant	ND	P-IF (NO)	>50.0	[116]
76	Xylorumpihiin I	TriT	Plant	3.9	P-IF (NO)	31.3	[116]
77	Xylorumpihiin J	TriT	Plant	3.9	P-IF (NO)	>50.0	[116]
78	Xylocensin X	TriT	Plant	2.5	P-IF (NO)	>50.0	[116]
79	Xylocensin E	TriT	Plant	1.5	P-IF (NO)	>50.0	[116]
80	Xylocensin K	TriT	Plant	1.9	P-IF (NO)	>50.0	[116]

Table A1. Cont.

N.	Terpene (T)				Inhibition (I)		
	Name	Class	Source	Log P <sup>1</sup>	Mechanism	IC <sub>50</sub> (μM) or I (%)	Refs.
81	Trichilin B	TriT	Plant	5.4	P-IF (NO)	29.2	[112]
82	3-Deacetyl-28-oxosalannin	TriT	Plant	3.1	P-IF (NO)	>100.0	[112]
83	3-Deacetyl-4'-demethyl-28-oxosalannin	TriT	Plant	ND	P-IF (NO)	>100.0	[112]
84	3-Deacetyl-28-oxosalannolactone	TriT	Plant	ND	P-IF (NO)	86.0	[112]
85	3-Deacetyl-28-oxoisosalanninolide	TriT	Plant	ND	P-IF (NO)	>100.0	[112]
86	3-Deacetyl-17-defurano-17,28-dioxosalannin	TriT	Plant	ND	P-IF (NO)	>100.0	[112]
87	Ohchinin	TriT	Plant	4.1	P-IF (NO)	28.7	[112]
88	23-Hydroxyohchininolide	TriT	Plant	ND	P-IF (NO)	58.6	[112]
89	21-Hydroxyisohchininolide	TriT	Plant	ND	P-IF (NO)	87.3	[112]
90	Gedunin	TriT	Plant	4.2	P-IF	ND	[78,117]
91	Lycopene	TetraT	Plant	15.6	P-IF	ND	[78,118]
92	Astaxanthin	TetraT	Algae	10.3	P-IF	ND	[78,119,120]
93	Carvone	MonoT	Plant	2.4	AChE	2900	[121]
94	Ocimene	MonoT	Plant	4.3	AChE	4700	[121]
95	Menthone	MonoT	Plant	2.7	AChE	9000	[121]
96	Pulegone	MonoT	Plant	2.8	AChE	9000	[121]
97	Citral	MonoT	Plant	3.0	AChE	IN	[121]
98	Citronellal	MonoT	Plant	3.0	AChE	IN	[121]
99	Terpinene-4-ol	MonoT	Plant	2.2	AChE	IN	[121]
100	β-Myrcene	MonoT	Plant	4.3	AChE	IN	[121]
101	γ-Terpinene	MonoT	Plant	2.8	AChE	IN	[121]
102	Isopulegol	MonoT	Plant	3.0	AChE	IN	[121]
103	Menthol	MonoT	Plant	3.0	AChE	IN	[121]
104	α-Terpinene	MonoT	Plant	4.2	AChE	IN	[121]
105	α-Phellandrene	MonoT	Plant	3.2	AChE	IN	[121]
106	Farnesene	SesquiT	Plant	5.7	AChE	ND	[121]
107	Cornigeraline A	SesquiT	Plant	ND	AChE	20.5	[114,122]
108	Sibthorpine	SesquiT	Plant	ND	AChE	35.8	[114]
109	3-Hydroxy-grosheimin	SesquiT	Plant	ND	AChE	30.5	[114]
110	Grosheimin	SesquiT	Plant	0.8	AChE	61.8	[114]
111	Solstitialin A	SesquiT	Plant	0.0	AChE	25.7	[114]
112	13-Chlorosolstitialine	SesquiT	Plant	ND	AChE	62.1	[114]
113	Cynaropicrin	SesquiT	Plant	0.6	AChE	31.3	[114]
114	1α,6β,8α-Triacetoxo-9β-furoyloxy-β-agarofuran	SesquiT	Plant	ND	AChE	248	[114,123]
115	1α-Hydroxy-6β,8α-diacetoxo-9β-furoyloxy-β-agarofuran	SesquiT	Plant	ND	AChE	738	[114,123]

Table A1. Cont.

N.	Terpene (T)				Inhibition (I)		
	Name	Class	Source	Log P <sup>1</sup>	Mechanism	IC <sub>50</sub> (μM) or I (%)	Refs.
116	1α,6β-Diacetoxy-8α-hydroxy-9β-furoyloxy-β-agarofuran	SesquiT	Plant	ND	AChE	161	[114,123]
117	1α-Acetoxy-6β,8α-dihydroxy-9β-furoyloxy-β-agarofuran	SesquiT	Plant	ND	AChE	312	[114,123]
118	1α,2α,6β,8α-Pentaacetoxy-9β-benzoyloxy-β-agarofuran	SesquiT	Plant	ND	AChE	122	[114,123]
119	1α,2α,3β,15-Tetraacetoxy-6β,9β-dibenzoyl-8-oxo-β-agarofuran	SesquiT	Plant	ND	AChE	463	[114,123]
120	1α,6β,15-Triacetoxy-9-benzoyloxy-β-agarofuran	SesquiT	Plant	ND	AChE	695	[114,123]
121	2α,3β,6β,8α,15-Pentaacetoxy-1α,9β-benzoyloxy-β-agarofuran	SesquiT	Plant	ND	AChE	482	[114,123]
122	1α-Acetoxy,6β,9β-difuroyloxy-4β-hydroxy-β-agarofuran	SesquiT	Plant	ND	AChE	738	[114,123]
123	Pulicaryenne A	SesquiT	Plant	ND	AChE	214.9	[124]
124	(1S,6R, 9S, 11R)-13,14-Dihydroxycaryophyll-2(15)-en-7-one	SesquiT	Plant	ND	AChE	40.0	[124]
125	(5Z)-14-Hydroxycaryophyllen-7-one	SesquiT	Plant	ND	AChE	108.3	[124]
126	(1S,6R, 9S, 11R)-13,14-Dihydroxycaryophyll-2(15)-en-7-one	SesquiT	Plant	ND	AChE	101.2	[124]
127	(1S,5Z,9R,11S)-12,14-Dihydroxycaryophylla-2(15),5-dien-7-one	SesquiT	Plant	ND	AChE	25.8	[124]
128	Quinanol A	SesquiT	Plant	ND	AChE	63.1% at 45 μM or 100.8 μM	[126]
129	Quinanol B	SesquiT	Plant	ND	AChE	15.0% at 45 μM	[126]
130	Quinanol C	SesquiT	Plant	ND	AChE	19.1% at 45 μM	[126]
131	Quinanol D	SesquiT	Plant	ND	AChE	<10% at 45 μM	[126]
132	Quinanol E	SesquiT	Plant	ND	AChE	<10% at 45 μM	[126]
133	Sinenofuranol	SesquiT	Plant	3.1	AChE	24.2% at 45 μM	[126]
134	Megatigma-7,9-diene-1,4-epoxy-2-hydroxy-10-carboxylic acid	SesquiT	Plant	ND	AChE	9.3	[127]
135	12-O-Demethylcryptojaponol	DiT	Plant	5.3	AChE	50.8	[114,128]
136	6α-Hydroxydemethylcryptojaponol	DiT	Plant	4.7	AChE	19.2	[114,128]
137	Lycosuarinone A	DiT	Plant	ND	AChE	26.8	[127]
138	15,16-Dihydrotanshinone	DiT	Plant	3.2	AChE	65.2% at 35.8 μM	[129]
139	Miltirone	DiT	Plant	4.9	AChE	IN	[129]
140	Cryptotanshinone	DiT	Plant	3.8	AChE	IN	[129]
141	1β-Hydroxy-cryptotanshinone	DiT	Plant	ND	AChE	IN	[129]
142	1,2-Didehydromiltirone	DiT	Plant	4.6	AChE	IN	[129]

Table A1. Cont.

N.	Terpene (T)				Inhibition (I)		
	Name	Class	Source	Log P <sup>1</sup>	Mechanism	IC <sub>50</sub> (μM) or I (%)	Refs.
143	Pentylcurcumene	DiT	Plant	ND	AChE	268.6	[130]
144	Serrat-14-en-3β,21α-diol	TriT	Plant	7.5	AChE	>50.0	[127]
145	Serrat-14-en-3β,21β-diol	TriT	Plant	7.5	AChE	>50.0	[127]
146	α-Onocerin	TriT	Plant	7.4	AChE	>50.0	[127]
147	26-Nor-8-oxo-α-onocerin	TriT	Plant	6.0	AChE	>50.0	[127]
148	26-Nor-8-oxo-21-one-α-onocerin	TriT	Plant	6.0	AChE	1.0	[127]
149	Colocynthenin A	TriT	Plant	2.7	AChE	2.6	[114,131]
150	Colocynthenin B	TriT	Plant	2.7	AChE	>10	[114,131]
151	Colocynthenin C	TriT	Plant	ND	AChE	3.1	[114,131]
152	Colocynthenin D	TriT	Plant	ND	AChE	>10.0	[114,131]
153	Cucurbitacin E	TriT	Plant	3.2	AChE	>10.0	[114,131]
154	6'-Acetyl-2-O-β-D-glucocucurbitacin E	TriT	Plant	ND	AChE	>10.0	[114,131]
155	Arvenin I	TriT	Plant	1.0	AChE	>10.0	[114,131]
156	Arvenin II	TriT	Plant	1.1	AChE	>10.0	[114,131]
157	Cucurbitacin B	TriT	Plant	2.6	AChE	>10.0	[114,131]
158	23,24-Dihydrocucurbitacin B	TriT	Plant	2.7	AChE	>10.0	[114,131]
159	Colocynthoside A	TriT	Plant	0.3	AChE	>10.0	[114,131]
160	Ganolucidic acid E	TriT	Plant	5.0	AChE	13.8	[114,132]
161	11β-Hydroxy-3,7-dioxo-5α-lanosta-8,24(E)-dien-26-oic acid	TriT	Plant	ND	AChE	10.8	[114,132]
162	23S-Hydroxy-3,7,11,15-tetraoxo-lanost-8,24(E)-diene-26-oic acid	TriT	Plant	ND	AChE	>200.0	[114,132]
163	Ganoderic acid X1	TriT	Plant	ND	AChE	>200.0	[114,132]
164	Ganoderenic acid D	TriT	Plant	2.0	AChE	>200.0	[114,132]
165	Ganoderenic acid H	TriT	Plant	2.7	AChE	>200.0	[114,132]
166	Ganoderic acid K	TriT	Plant	2.2	AChE	>200.0	[114,132]
167	3β,7β-Dihydroxy-11,15,23-trioxo-lanost-8,16-dien-26-oic acid	TriT	Plant	1.9	AChE	>200.0	[114,132]
168	Ganoderic acid E	TriT	Plant	2.3	AChE	>200.0	[114,132]
169	12-Acetoxy-3,7,11,15,23-pentaoxolanost-8,20-dien-26-oic acid	TriT	Plant	ND	AChE	>200.0	[114,132]
170	7β-Hydroxy-3,11,15,23-tetraoxo-27ξ-lanost-8,16-dien-26-oic acid	TriT	Plant	ND	AChE	>200.0	[114,132]
171	Ganoderenic acid B	TriT	Plant	2.4	AChE	>200.0	[114,132]
172	Ganoderenic acid F	TriT	Plant	2.4	AChE	>200.0	[114,132]
173	Ganodernoid D	TriT	Plant	2.1	AChE	>200.0	[114,132]
174	Ganodernoid F	TriT	Plant	2.1	AChE	>200.0	[114,132]
175	Ganoderenic acid C	TriT	Plant	2.7	AChE	>200.0	[114,132]

Table A1. Cont.

N.	Terpene (T)			Log P <sup>1</sup>	Mechanism	Inhibition (I)	
	Name	Class	Source			IC <sub>50</sub> (μM) or I (%)	Refs.
176	3β-Hydroxyganoderoid D	TriT	Plant	2.4	AChE	>200.0	[114,132]
177	Ganoderic acid H	TriT	Plant	2.6	AChE	>200.0	[114,132]
178	12β-Hydroxyganoderenic acid F	TriT	Plant	1.9	AChE	>200.0	[114,132]
179	Methylganoderate F	TriT	Plant	ND	AChE	>200.0	[114,132]
180	Ganoderic acid J	TriT	Plant	2.6	AChE	>200.0	[114,132]
181	Ganoderic acid F	TriT	Plant	2.3	AChE	>200.0	[114,132]
182	Ganoderic acid AP	TriT	Plant	ND	AChE	>200.0	[114,132]
183	Ganoderic acid B	TriT	Plant	2.2	AChE	>200.0	[114,132]
184	Ganoderic acid C	TriT	Plant	2.5	AChE	>200.0	[114,132]
185	Ganoderic acid D	TriT	Plant	1.9	AChE	>200.0	[114,132]
186	Ganoderic acid G	TriT	Plant	1.7	AChE	>200.0	[114,132]
187	Ganoderic acid N	TriT	Plant	0.7	AChE	>200.0	[114,132]
188	Methyl ganoderate G	TriT	Plant	2.9	AChE	>200.0	[114,132]
189	Ganoderic acid Am1	TriT	Plant	ND	AChE	183.0	[114,132]
190	Methyl ganoderate C	TriT	Plant	2.2	AChE	148.0	[114,132]
191	Ganoderoid C1	TriT	Plant	ND	AChE	142.0	[114,132]
192	12β-Hydroxyganoderenic acid F	TriT	Plant	ND	AChE	102.0	[114,132]
193	Methyl ganoderate E	TriT	Plant	2.6	AChE	45.8	[114,132]
194	Ganoderic acid C6	TriT	Plant	2.0	AChE	147.5	[114,132]
195	Methyl ganoderic acid C6	TriT	Plant	ND	AChE	145.2	[114,132]
196	Gaoderoid A	TriT	Plant	ND	AChE	149.0	[114,132]
197	Gaoderoid B2	TriT	Plant	ND	AChE	102.4	[114,132]
198	Ganoderlactone G	TriT	Plant	ND	AChE	130.5	[114,132]
199	Lucidone A	TriT	Plant	1.2	AChE	>200.0	[114,132]
200	Lucidone D	TriT	Plant	2.4	AChE	>200.0	[114,132]
201	Ganoderoid B	TriT	Plant	1.5	AChE	>200.0	[114,132]
202	Ganodermanondiol	TriT	Plant	5.8	AChE	>200.0	[114,132]
203	Norfriedelin A	TriT	Plant	7.6	AChE	10.3	[114,133]
204	Norfriedelin B	TriT	Plant	8.3	AChE	28.7	[114,133]
205	Norfriedelin C	TriT	Plant	7.9	AChE	>50.0	[114,133]
206	3β-Hydroxy-24-nor-urs-4(23)-12-dien-28-oic acid	TriT	Plant	ND	AChE	10.0	[113,114]
207	Euscaphic acid	TriT	Plant	5.0	AChE	35.9	[114,134]
208	Arjunic acid	TriT	Plant	5.2	AChE	37.5	[114,134]
209	Ursolic acid	TriT	Plant	7.3	AChE	21.5	[114,134]
210	2-Hydroxy-3α-O-caffeoyltaraxar-14-en-28-oic acid	TriT	Plant	ND	AChE	13.5	[114,135]
211	Taraxerol	TriT	Plant	9.3	AChE	ND	[114,135]
212	Betulin	TriT	Plant	8.3	AChE	28.5	[114,135]

Table A1. Cont.

N.	Terpene (T)				Inhibition (I)		
	Name	Class	Source	Log <i>P</i> <sup>1</sup>	Mechanism	IC <sub>50</sub> (μM) or I (%)	Refs.
213	Betulinic acid	TriT	Plant	8.2	AChE	24.2	[114,135]
214	Asperversin A	MeroT	Fungus	2.3	AChE	>40.0	[136]
215	Asperversin B	MeroT	Fungus	2.2	AChE	>40.0	[136]
216	Asperversin C	MeroT	Fungus	3.4	AChE	>40.0	[136]
217	Asperversin D	MeroT	Fungus	2.4	AChE	>40.0	[136]
218	Asperversin E	MeroT	Fungus	2.0	AChE	>40.0	[136]
219	Asperversin F	MeroT	Fungus	2.6	AChE	>40.0	[136]
220	Asperdemin	MeroT	Fungus	1.4	AChE	>40.0	[136]
221	Asperversin G	MeroT	Fungus	3.3	AChE	13.6	[136]

<sup>1</sup> Log *P*-values from the chemical databases PubChem and ChemSpider. Legend: IN–no activity; ND–not-determined; P-IF–proinflammatory factor.

## References

1. Shabab, T.; Khanabdali, R.; Moghadamtousi, S.Z.; Kadir, H.A.; Mohan, G. Neuroinflammation pathways: A general review. *Int. J. Neurosci.* **2017**, *127*, 624–633. [[CrossRef](#)] [[PubMed](#)]
2. Livingston, G.; Huntley, J.; Sommerlad, A.; Ames, D.; Ballard, C.; Banerjee, S.; Brayne, C.; Burns, A.; Cohen-Mansfield, J.; Cooper, C.; et al. Dementia prevention, intervention, and care: 2020 report of the Lancet Commission. *Lancet* **2020**, *396*, 413–446. [[CrossRef](#)] [[PubMed](#)]
3. Alzheimer's Association. Alzheimer's disease facts and figures. *Alzheimer's Dement.* **2019**, *15*, 321–387.
4. Isik, A.T. Late onset Alzheimer's disease in older people. *Clin. Interv. Aging* **2010**, *5*, 307–311. [[CrossRef](#)] [[PubMed](#)]
5. Van Cauwenberghe, C.; van Broeckhoven, C.; Sleegers, K. The genetic landscape of Alzheimer disease: Clinical implications and perspectives. *Genet. Med.* **2016**, *18*, 421–430. [[CrossRef](#)]
6. Hauser, P.S.; Narayanaswami, V.; Ryan, R.O. Apolipoprotein E: From lipid transport to neurobiology. *Prog. Lipid Res.* **2011**, *50*, 62–74. [[CrossRef](#)] [[PubMed](#)]
7. Liu, C.; Kanekiyo, T.; Xu, H.; Bu, G. Apolipoprotein E and Alzheimer disease: Risk, mechanisms and therapy. *Nat. Rev. Neurol.* **2013**, *9*, 106–118. [[CrossRef](#)] [[PubMed](#)]
8. Kim, J.; Basak, J.M.; Holtzman, D.M. The role of apolipoprotein E in Alzheimer's disease. *Neuron* **2009**, *63*, 287–303. [[CrossRef](#)] [[PubMed](#)]
9. Shi, Y.; Yamada, K.; Liddel, S.A.; Smith, S.T.; Zhan, L.; Lun, W.; Tsai, R.M.; Spina, S.; Grinberg, L.T.; Rojas, J.C.; et al. ApoEε4 markedly exacerbates tau-mediated neurodegeneration in a mouse model of tauopathy. *Nature* **2017**, *549*, 523–527. [[CrossRef](#)]
10. Bekris, L.M.; Yu, C.; Bird, T.D.; Tsuang, T.W. Genetics of Alzheimer's disease. *J. Geriatr. Psychiatry Neurol.* **2010**, *23*, 213–227. [[CrossRef](#)]
11. Martins, M.; Silva, R.; Pinto, M.M.M.; Sousa, E. Marine natural products, multitarget therapy and repurposed agents in Alzheimer's disease. *Pharmaceuticals* **2020**, *13*, 242. [[CrossRef](#)]
12. Anand, P.; Singh, B.; Singh, N. A review on coumarins as acetylcholinesterase inhibitors for Alzheimer's disease. *Bioorg. Med. Chem.* **2012**, *20*, 1175–1180. [[CrossRef](#)]
13. Macauley, S.L.; Holtzman, D.M. Recent advances from the bench toward the bedside in Alzheimer's disease. *EBioMedicine* **2015**, *2*, 94–95. [[CrossRef](#)]
14. Takashima, A. Tau aggregation is a therapeutic target for Alzheimer's disease. *Curr. Alzheimer Res.* **2010**, *7*, 665–669. [[CrossRef](#)]
15. Coman, H.; Nemes, B. New therapeutic targets in Alzheimer's disease. *Int. J. Gerontol.* **2017**, *11*, 2–6. [[CrossRef](#)]
16. Cummings, J.L.; Tong, G.; Ballard, C. Treatment combinations for Alzheimer's disease: Current and future pharmacotherapy options. *J. Alzheimer's Dis.* **2019**, *67*, 779–794. [[CrossRef](#)]
17. Fish, P.V.; Steadman, D.; Bayle, E.D.; Whiting, P. New approaches for the treatment of Alzheimer's disease. *Bioorg. Med. Chem. Lett.* **2019**, *29*, 125–133. [[CrossRef](#)]
18. Desai, A.; Mitchison, T.J. Microtubule polymerization dynamics. *Annu. Rev. Cell Dev. Biol.* **1997**, *13*, 83–117. [[CrossRef](#)] [[PubMed](#)]
19. Mitchison, T.; Kirschner, M. Dynamic instability of microtubule growth. *Nature* **1984**, *312*, 237–242. [[CrossRef](#)]
20. Ballatore, C.; Brunden, K.R.; Hurn, D.M.; Trojanowski, J.Q.; Lee, V.M.-Y.; Smith, A.B., III. Microtubule stabilizing agents as potential treatment for Alzheimer's disease and related neurodegenerative tauopathies. *J. Med. Chem.* **2012**, *55*, 8979–8996. [[CrossRef](#)]
21. White, J.A., II; Banerjee, R.; Gunawardena, S. Axonal transport and neurodegeneration: How marine drugs can be used for the development of therapeutics. *Mar. Drugs* **2016**, *14*, 102. [[CrossRef](#)] [[PubMed](#)]
22. Kosik, K.S.; Joachim, C.L.; Selkoe, D.J. Microtubule-associated protein tau (tau) is a major antigenic component of paired helical filaments in Alzheimer disease. *Proc. Natl. Acad. Sci. USA* **1986**, *83*, 4044–4048. [[CrossRef](#)] [[PubMed](#)]
23. Naini, S.; Soussi-Yanicostas, N. Tau hyperphosphorylation and oxidative stress, a critical vicious circle in neurodegenerative tauopathies? *Oxidative Med. Cell. Longev.* **2015**, *2015*, 151979.
24. Kolarova, M.; García-Sierra, F.; Bartos, A.; Ricny, J.; Ripava, D.; Ripava, D. Structure and pathology of tau protein in Alzheimer disease. *Int. J. Alzheimer's Dis.* **2012**, *2012*, 731526. [[CrossRef](#)] [[PubMed](#)]
25. Martin, L.; Latypova, X.; Wilson, C.M.; Magnaudeix, A.; Perrin, M.-L.; Yarden, C.; Terra, F. Tau protein kinases: Involvement in Alzheimer's disease. *Ageing Res. Rev.* **2013**, *12*, 289–309. [[CrossRef](#)]
26. Citron, M. Alzheimer's disease: Strategies for disease modification. *Nat. Rev. Drug Discov.* **2010**, *9*, 387–398. [[CrossRef](#)] [[PubMed](#)]
27. Li, G.; Yin, H.; Kuret, J. Casein kinase 1 delta phosphorylates tau and disrupts its binding to microtubules. *J. Biol. Chem.* **2004**, *279*, 15938–15945. [[CrossRef](#)] [[PubMed](#)]
28. Llorach-Pares, L.; Nonell-Canals, A.; Avila, C.; Sanchez-Martinez, M. Kororamides, convolutamines, and indole derivatives as possible tau and dual-specificity kinase inhibitors for Alzheimer's disease: A computational study. *Mar. Drugs* **2018**, *16*, 386. [[CrossRef](#)] [[PubMed](#)]
29. Jain, P.; Karthikeyan, C.; Moorthy, H.N.; Waiker, D.K.; Jain, A.K.; Trivedi, P. Human CDC2-like kinase 1 (CLK1): A novel target for Alzheimer's disease. *Curr. Drug Targets* **2014**, *15*, 539–550. [[CrossRef](#)]
30. Tell, V.; Hilgeroth, A. Recent developments of protein kinase inhibitors as potential AD therapeutics. *Front. Cell. Neurosci.* **2013**, *7*, 189. [[CrossRef](#)]
31. Dolan, P.J.; Johnson, G.V.W. The role of tau kinases in Alzheimer's disease. *Curr. Opin. Drug Discov. Dev.* **2010**, *13*, 595–603.

32. Stotani, S.; Giordanetto, F.; Medda, F. DYRK1A inhibition as potential treatment for Alzheimer's disease. *Future Med. Chem.* **2016**, *8*, 681–696. [[CrossRef](#)] [[PubMed](#)]
33. Branca, C.; Shaw, D.M.; Belfiore, R.; Gokhale, V.; Shaw, A.Y.; Foley, C.; Smith, B.; Hulme, C.; Dunckley, T.; Meechoovet, B.; et al. Dyrkl inhibition improves Alzheimer's disease-like pathology. *Aging Cell* **2017**, *16*, 1146–1154. [[CrossRef](#)] [[PubMed](#)]
34. Hooper, C.; Killick, R.; Lovestone, S. The GSK3 hypothesis of Alzheimer's disease. *J. Neurochem.* **2008**, *104*, 1433–1439. [[CrossRef](#)] [[PubMed](#)]
35. Llorens-Martín, M.; Jurado, J.; Hemández, F.; Avila, J. GSK-3, a pivotal kinase in Alzheimer disease. *Front. Mol. Neurosci.* **2014**, *7*, 46. [[CrossRef](#)]
36. Hemández, F.; Gómez de Barreda, E.; Fuster-Matanzo, A.; Lucas, J.J.; Avila, J. GSK3: A possible link between beta amyloid peptide and tau protein. *Exp. Neurol.* **2010**, *223*, 322–325. [[CrossRef](#)] [[PubMed](#)]
37. Hemández, F.; Lucas, J.J.; Avila, J. GSK3 and tau: Two convergence points in Alzheimer's disease. *J. Alzheimers Dis.* **2013**, *33* (Suppl. S1), S141–S144. [[CrossRef](#)]
38. Heneka, M.T.; Kummer, M.P. Innate immune activation in neurodegenerative disease. *Nat. Rev. Immunol.* **2014**, *14*, 463–477. [[CrossRef](#)]
39. Schain, M.; Kreisler, W.C. Neuroinflammation in neurodegenerative disorders: A review. *Curr. Neurol. Neurosci. Rep.* **2017**, *17*, 25. [[CrossRef](#)]
40. Barbalace, M.C.; Malaguti, M.; Giusti, L.; Lucacchini, A.; Hrelia, S.; Angeloni, C. Anti-inflammatory activities of marine algae in neurodegenerative diseases. *Int. J. Mol. Sci.* **2019**, *20*, 3061. [[CrossRef](#)]
41. Salter, M.W.; Stevens, B. Microglia emerge as central players in brain disease. *Nat. Med.* **2017**, *23*, 1018–1027. [[CrossRef](#)]
42. Cowan, M.; Petri, W.A. Microglia: Immune regulators of neurodevelopment. *Front. Immunol.* **2018**, *9*, 2576. [[CrossRef](#)] [[PubMed](#)]
43. Hansen, D.V.; Hanson, J.E.; Sheng, M. Microglia in Alzheimer's disease. *J. Cell. Biol.* **2018**, *217*, 459–472. [[CrossRef](#)]
44. Colonna, M.; Butovsky, O. Microglia function in the central nervous system during health and neurodegeneration. *Annu. Rev. Immunol.* **2017**, *35*, 44–468. [[CrossRef](#)]
45. Dong, Y.; Li, X.; Cheng, J.; Hou, L. Drug development for Alzheimer's disease: Microglia induced neuroinflammation as a target? *Int. J. Mol. Sci.* **2019**, *20*, 558. [[CrossRef](#)] [[PubMed](#)]
46. Liu, C.Y.; Wang, X.; Liu, C.; Zhang, H.L. Pharmacological targeting of microglial activation: New therapeutic approach. *Front. Cell. Neurosci.* **2019**, *13*, 514. [[CrossRef](#)]
47. Anglister, L.; Stiles, J.R.; Salpeter, M.M. Acetylcholinesterase density and turnover number at frog neuromuscular-junctions, with modeling of their role in synaptic function. *Neuron* **1994**, *12*, 783–794. [[CrossRef](#)]
48. Ferreira-Vieira, T.H.; Guimaraes, I.M.; Silva, F.R.; Ribeiro, F.M. Alzheimer's disease: Targeting the cholinergic system. *Curr. Neuropharmacol.* **2016**, *14*, 101–111. [[CrossRef](#)] [[PubMed](#)]
49. Houghton, P.J.; Ren, Y.; Howes, M. Acetylcholinesterase inhibitors from plants and fungi. *J. Nat. Prod. Rep.* **2006**, *23*, 181–199. [[CrossRef](#)]
50. Inestrosa, N.C.; Alvarez, A.; Perez, C.A.; Moreno, R.D.; Vicente, M.; Linker, C.; Casanueva, O.I.; Soto, C.; Garrido, J. Acetylcholinesterase accelerates assembly of amyloid- $\beta$ -peptides into Alzheimer's fibrils: Possible role of the peripheral site of the enzyme. *Neuron* **1996**, *16*, 881–889. [[CrossRef](#)]
51. Alvarez, A.; Alarcón, R.; Opazo, C.; Campos, E.O.; Muñoz, F.J.; Calderón, F.H.; Dajas, F.; Gentry, M.K.; Doctor, B.P.; De Mello, F.G.; et al. Stable complexes involving acetylcholinesterase and amyloid-beta peptide change the biochemical properties of the enzyme and increase the neurotoxicity of Alzheimer's fibrils. *J. Neurosci.* **1998**, *18*, 3213–3223. [[CrossRef](#)] [[PubMed](#)]
52. Chen, J.J.; Genereux, J.C.; Wiseman, R.L. Endoplasmic reticulum quality control and systemic amyloid disease: Impacting protein stability from the inside out. *IUBMB Life* **2015**, *67*, 404–413. [[CrossRef](#)] [[PubMed](#)]
53. Wang, T.; Liu, X.H.; Guan, J.; Ge, S.; Wu, M.B.; Lin, J.P. Advancement of multi-target drug discoveries and promising applications in the field of Alzheimer's disease. *Eur. J. Med. Chem.* **2019**, *169*, 200–223. [[CrossRef](#)] [[PubMed](#)]
54. Cho, K.S.; Lim, Y.; Lee, K.; Lee, J.; Lee, J.H.; Lee, I.-S. Terpenes from forests and human health. *Toxicol. Res.* **2017**, *33*, 97–106. [[CrossRef](#)] [[PubMed](#)]
55. Wang, Y.; Huang, L.Q.; Tang, X.C.; Zhang, H.Y. Retrospect and prospect of active principles from Chinese herbs in the treatment of dementia. *Acta Pharmacol. Sin.* **2010**, *31*, 649–664. [[CrossRef](#)] [[PubMed](#)]
56. Prado-Audelo, M.L.; Cortés, H.; Caballero-Florán, I.H.; González-Torres, M.; Escutia-Guadarrama, L.; Sergio, A.; Bernal-Chávez, S.A.; Giraldo-Gomez, D.M.; Magaña, J.J.; Leyva-Gómez, G. Therapeutic applications of terpenes on inflammatory diseases. *Front. Pharmacol.* **2021**, *12*, 704197. [[CrossRef](#)] [[PubMed](#)]
57. Geris, R.; Simpson, T.J. Meroterpenoids produced by fungi. *Nat. Prod. Rep.* **2009**, *26*, 1063–1094. [[CrossRef](#)]
58. Ninkuu, V.; Zhang, L.; Yan, J.; Fu, Z.; Yang, T.; Zeng, H. Biochemistry of terpenes and recent advances in plant protection. *Int. J. Mol. Sci.* **2021**, *22*, 5710. [[CrossRef](#)]
59. Bodor, N.; Buchwald, P. *Retrometabolic Drug Design and Targeting*; John Wiley & Sons: Hoboken, NJ, USA, 2012; pp. 9–38.
60. Leeson, P.D.; Springthorpe, B. The influence of drug-like concepts on decision-making in medicinal chemistry. *Nat. Rev. Drug Discov.* **2007**, *11*, 881–890. [[CrossRef](#)]
61. Youdim, K.A.; Dobbie, M.S.; Kuhnle, G.; Proteggente, A.R.; Abbott, N.J.; Rice-Evans, C. Interaction between flavonoids and the blood-brain barrier: In vitro studies. *J. Neurochem.* **2003**, *85*, 180–192. [[CrossRef](#)]

62. Muralidharan, A.; Josyula, V.R.; Hariharapura, R.C. Exploring the potential of marine microbes in clinical management of Alzheimer's disease: A road map for bioprospecting and identifying promising isolates. *Life Sci.* **2018**, *208*, 149–160. [[CrossRef](#)] [[PubMed](#)]
63. Videira, R.; Castanheira, P.; Grãos, M.; Salgueiro, L.; Faro, C.; Cavaleiro, C. A necrodane monoterpene from *Lavandula luisieri* essential oil as a cell-permeable inhibitor of BACE-1, the  $\beta$ -secretase in Alzheimer's disease. *Flavour Fragr. J.* **2013**, *28*, 380–388. [[CrossRef](#)]
64. Naushad, M.; Durairajan, S.S.K.; Bera, A.K.; Senapati, S.; Li, M. Natural compounds with anti-BACE1 as promising therapeutic drugs for treating Alzheimer's disease. *Planta Med.* **2019**, *85*, 1316–1325. [[PubMed](#)]
65. Leirós, M.; Alonso, E.; Rateb, M.E.; Houssen, W.E.; Ebel, R.; Jaspars, M.; Alfonso, A.; Botana, L.M. Gracilins: *Spongionella*-derived promising compounds for Alzheimer's disease. *Neuropharmacology* **2015**, *93*, 285–293. [[CrossRef](#)] [[PubMed](#)]
66. Wang, Y.-H.; Du, G.-H. Ginsenoside Rg1 inhibits  $\beta$ -secretase activity in vitro and protects against A $\beta$ -induced cytotoxicity in PC12 cells. *J. Asian Nat. Prod. Res.* **2009**, *11*, 604–612. [[CrossRef](#)] [[PubMed](#)]
67. Cao, G.; Su, P.; Zhang, S.; Guo, L.; Zhang, H.; Liang, Y.; Qin, C.; Zhang, W. Ginsenoside Re reduces A $\beta$  production by activating PPAR $\gamma$  to inhibit BACE1 in N2a/APP695 cells. *Eur. J. Pharmacol.* **2016**, *793*, 101–110. [[CrossRef](#)]
68. Chen, F.; Eckman, E.A.; Eckman, C.B. Reductions in levels of the Alzheimer's amyloid  $\beta$  peptide after oral administration of ginsenosides. *FASEB J.* **2006**, *20*, 1269–1271. [[CrossRef](#)]
69. Laws, J.S., 3rd; Smid, S.D. Evaluating *Cannabis sativa* L.'s neuroprotection potential: From bench to bedside. *Phytomedicine* **2022**, *107*, 154485. [[CrossRef](#)] [[PubMed](#)]
70. Zhen, Z.; Jingyu, Y.; Chen, L.; Jun, X.; Shi, Q.; Xue, Y.; Chunfu, W. Pseudoginsenoside-F11 alleviates cognitive deficits and Alzheimer's disease-type pathologies in SAMP8 mice. *Pharmacol. Res.* **2019**, *139*, 512–523.
71. Fischbach, M.A.; Walsh, C.T. Assembly-line enzymology for polyketide and nonribosomal peptide antibiotics: Logic, machinery, and mechanisms. *Chem. Rev.* **2006**, *106*, 3468–3496. [[CrossRef](#)]
72. Itoh, T.; Tokunaga, K.; Matsuda, Y.; Fujii, I.; Abe, I.; Ebizuka, Y.; Kushiro, T. Reconstitution of a fungal meroterpenoid biosynthesis reveals the involvement of a novel family of terpene cyclases. *Nat. Chem.* **2010**, *2*, 858–864. [[CrossRef](#)] [[PubMed](#)]
73. Qi, C.; Bao, J.; Wang, J.; Zhu, H.; Xue, Y.; Wang, X.; Li, H.; Sun, W.; Gao, W.; Lai, Y.; et al. Asperterpenes A and B, two unprecedented meroterpenoids from *Aspergillus terreus* with BACE1 inhibitory activities. *Chem. Sci.* **2016**, *7*, 6563. [[CrossRef](#)] [[PubMed](#)]
74. Qi, C.; Liu, M.; Zhou, Q.; Gao, W.; Chen, C.; Lai, Y.; Hu, Z.; Xue, Y.; Zhang, J.; Li, D.; et al. BACE1 Inhibitory meroterpenoids from *Aspergillus terreus*. *J. Nat. Prod.* **2018**, *81*, 1937–1945. [[CrossRef](#)]
75. Qi, C.; Qiao, Y.; Gao, W.; Liu, M.; Zhou, Q.; Chen, C.; Lai, Y.; Xue, Y.; Zhang, J.; Li, D.; et al. New 3,5-dimethylorsellinic acid-based meroterpenoids with BACE1 and AchE inhibitory activities from *Aspergillus terreus*. *Org. Biomol. Chem.* **2018**, *16*, 9046. [[CrossRef](#)] [[PubMed](#)]
76. Nguyen, V.T.; To, D.C.; Tran, M.H.; Oh, S.H.; Kim, J.A.; Ali, M.Y.; Woo, M.-H.; Choi, J.S.; Min, B.S. Isolation of cholinesterase and  $\beta$ -secretase 1 inhibiting compounds from *Lycopodiella cernua*. *Bioorg. Med. Chem.* **2015**, *23*, 3126–3134. [[CrossRef](#)] [[PubMed](#)]
77. Shin, M.; Liu, Q.F.; Choi, B.; Shin, C.; Lee, B.; Yuan, C.; Song, Y.J.; Yun, H.S.; Lee, I.-S.; Koo, B.-S.; et al. Neuroprotective effects of limonene (+) against A $\beta$ 42-induced neurotoxicity in a *Drosophila* Model of Alzheimer's Disease. *Biol. Pharm. Bull.* **2020**, *43*, 409–417. [[CrossRef](#)] [[PubMed](#)]
78. Fakhri, S.; Pesce, M.; Patruno, A.; Moradi, S.Z.; Iranpanah, A.; Farzaei, M.H.; Sobarzo-Sanchez, E. Attenuation of NrF<sub>2</sub>/Keap<sub>1</sub>/ARE in Alzheimer's disease by plant secondary metabolites: A mechanistic review. *Molecules* **2020**, *25*, 4926. [[CrossRef](#)] [[PubMed](#)]
79. Yuan, C.; Shin, M.; Park, Y.; Choi, B.; Jang, S.; Lim, C.; Yun, H.S.; Lee, I.-S.; Won, S.-Y. Linalool alleviates A $\beta$ 42-Induced neurodegeneration via suppressing ROS production and inflammation in fly and rat models of Alzheimer's disease. *Oxidative Med. Cell. Longev.* **2021**, *2021*, 8887716. [[CrossRef](#)] [[PubMed](#)]
80. Efferth, T.; Oesch, F. The immunosuppressive activity of artemisin-type drugs towards inflammatory and auto immune diseases. *Med. Res. Rev.* **2021**, *41*, 3023–3061. [[CrossRef](#)]
81. Abulfadl, Y.S.; El-Maraghy, N.N.; Ahmed, A.E.; Nofal, S.; Abdel-Mottaleb, Y.; Badary, O.A. Thymoquinone alleviates the experimentally induced Alzheimer's disease inflammatory by modulation of TLRs signaling. *Hum. Exp. Toxicol.* **2018**, *37*, 1092–1104. [[CrossRef](#)]
82. Krylova, N.G.; Drobysch, M.S.; Semenkova, G.N.; Kulahava, T.A.; Pinchuk, S.V.; Shadyro, O.I. Cytotoxic and antiproliferative effects of thymoquinone on rat C6 glioma cells depend on oxidative stress. *Mol. Cell. Biochem.* **2019**, *462*, 195–206. [[CrossRef](#)] [[PubMed](#)]
83. Wang, P.; Luo, Q.; Qiao, H.; Ding, H.; Cao, Y.; Yu, J.; Liu, R.; Zhang, Q.; Zhu, H.; Qu, I. The neuroprotective effects of ethanol-induced hippocampal neurons impairment via the antioxidative and antipoptotic pathways. *Oxidative Med. Cell. Longev.* **2017**, *2017*, 4079425. [[PubMed](#)]
84. Porres-Martínez, M.; González-Burgos, E.; Carretero, M.E.; Gómez-Serranillos, M.P. In vitro neuroprotective potential of the monoterpenes  $\alpha$ -pinene and 1,8-cineole against H<sub>2</sub>O<sub>2</sub>-induced oxidative stress in PC12 cells. *Z. Naturforsch. C J. Biosci.* **2016**, *71*, 191–199. [[CrossRef](#)] [[PubMed](#)]
85. Oliveira, T.M.; Carvalho, R.B.F.; Costa, I.H.F.; Oliveira, G.A.L.; Souza, A.A.; Lima, S.G.; Freitas, R.M. Evaluation of *p*-cymene, a natural antioxidant. *Pharm. Biol.* **2015**, *53*, 423–428. [[CrossRef](#)] [[PubMed](#)]

86. Pires, L.F.; Costa, L.M.; Almeida, A.A.C.; Silva, O.A.; Cerqueira, G.S.; Sousa, D.P.; Freitas, R.M. Is there a correlation between in vitro antioxidant potential and in vivo effect of carvacryl acetate against oxidative stress in mice hippocampus? *Neurochem. Res.* **2014**, *39*, 758–769. [[CrossRef](#)] [[PubMed](#)]
87. Hur, J.; Pak, S.C.; Koo, B.-S.; Jeon, S. Borneol alleviates oxidative stress via upregulation of Nrf2 and Bcl-2 in SH-SY5Y cells. *Pharm. Biol.* **2013**, *51*, 30–35. [[CrossRef](#)] [[PubMed](#)]
88. Prasad, S.N.; Muralidhara, M. Analysis of the antioxidant activity of geraniol employing various in vitro models. Relevance to neurodegeneration in diabetic neuropathy. *Asian J. Pharm. Clin. Res.* **2017**, *10*, 10–105. [[CrossRef](#)]
89. Olajide, O.A.; Sarker, S.D. Alzheimer's disease: Natural products as inhibitors of neuroinflammation. *Inflammopharmacology* **2020**, *28*, 1439–1455. [[CrossRef](#)] [[PubMed](#)]
90. Souček, M.; Herout, V.; Šorm, F. On terpenes CXVIII. Constitution of parthenolide. *Collect. Czech. Chem. Commun.* **1961**, *26*, 803–810. [[CrossRef](#)]
91. Lee, J.; Songa, K.; Huhb, E.; Oh, M.S.; Kima, Y.S. Neuroprotection against 6-OHDA toxicity in PC12 cells and mice through the Nrf2 pathway by a sesquiterpenoid from *Tussilago farfara*. *Redox Biol.* **2018**, *18*, 6–15. [[CrossRef](#)]
92. Ramu Venkatesan, R.; Subedi, L.; Yeo, E.-J.; Kim, S.Y. Lactucopicrin ameliorates oxidative stress mediated by scopolamine-induced neurotoxicity through activation of the NRF2 pathway. *Neurochem. Int.* **2016**, *99*, 133–146. [[CrossRef](#)] [[PubMed](#)]
93. Huang, B.X.; He, D.W.; Chen, G.X.; Ran, X.; Guo, W.J.; Kan, X.C.; Wang, W.; Liu, D.F.; Fu, S.P.; Liu, J.X.  $\alpha$ -Cyperone inhibits LPS-induced inflammation in BV-2 cells through activation of Akt/Nrf2/HO-1 and suppression of the NF- $\kappa$ B pathway. *Food Funct.* **2018**, *9*, 2735–2743. [[CrossRef](#)] [[PubMed](#)]
94. Park, S.Y.; Choi, M.H.; Park, G.; Choi, Y.-W. *Petasites japonicus* bakkenolide B inhibits lipopolysaccharide-induced pro-inflammatory cytokines via AMPK/Nrf2 induction in microglia. *Int. J. Molec. Med.* **2018**, *41*, 1683–1692. [[CrossRef](#)] [[PubMed](#)]
95. Deng, M.; Yan, W.; Gu, Z.; Li, Y.; Chen, L.; He, B. Anti-neuroinflammatory potential of natural products in the treatment of Alzheimer's disease. *Molecules* **2023**, *28*, 1486. [[CrossRef](#)] [[PubMed](#)]
96. Satoh, T.; Trudler, D.; Oh, C.K.; Lipton, S.A. Potential therapeutic use of the Rosemary diterpene carnosic acid for Alzheimer's disease, Parkinson's disease, and long-COVID through NRF2 activation to counteract the NLRP3 inflammasome. *Antioxidants* **2022**, *11*, 124. [[CrossRef](#)] [[PubMed](#)]
97. Hebert, M.; Bellavance, G.; Barriault, L. Total synthesis of ginkgolide C and formal synthesis of ginkgolides A and B. *J. Am. Chem. Soc.* **2022**, *144*, 17792–17796. [[CrossRef](#)] [[PubMed](#)]
98. Liu, X.G.; Lu, X.; Gao, W.; Li, P.; Yang, H. Structure, synthesis, biosynthesis, and activity of the characteristic compounds from *Ginkgo biloba* L. *Nat. Prod. Rep.* **2022**, *39*, 474–511. [[CrossRef](#)] [[PubMed](#)]
99. Niu, T.T.; Yin, H.; Xu, B.L.; Yang, T.T.; Li, H.Q.; Sun, Y.; Liu, G.Z. Protective effects of ginkgolide on a cellular model of Alzheimer's disease via suppression of the NF- $\kappa$ B signaling pathway. *Appl. Biochem. Biotechnol.* **2022**, *194*, 2448–2464. [[CrossRef](#)] [[PubMed](#)]
100. Lv, Z.; Yang, Y.; Wang, J.; Chen, J.; Li, J.; Di, L. Optimization of the preparation conditions of borneol-modified ginkgolide liposomes by response surface methodology and study of their blood brain barrier permeability. *Molecules* **2018**, *23*, 303. [[CrossRef](#)]
101. Leirós, M.; Sánchez, J.A.; Alonso, E.; Rateb, M.E.; Houssen, W.E.; Ebel, R.; Jaspars, M.; Alfonso, A.; Botana, L.M. *Spongionella* secondary metabolites protect mitochondrial function in cortical neurons against oxidative stress. *Mar. Drugs* **2014**, *12*, 700–718. [[CrossRef](#)]
102. Lee, B.; Sur, B.; Park, J.; Kim, S.H.; Kwon, S.; Yeom, M.; Shim, I.; Lee, H.; Hahm, D.H. Ginsenoside Rg3 alleviates lipopolysaccharide-induced learning and memory impairments by anti-inflammatory activity in rats. *Biomol. Ther.* **2013**, *21*, 381–390. [[CrossRef](#)]
103. Ahn, J.W.; Jang, S.K.; Jo, B.R.; Kim, H.S.; Park, J.Y.; Park, H.Y.; Yoo, Y.M.; Joo, S.S. A therapeutic intervention for Alzheimer's disease using ginsenoside Rg3: Its role in M2 microglial activation and non-amyloidogenesis. *J. Physiol. Pharmacol.* **2021**, *72*, 185–193.
104. Li, J.; Huang, Q.; Chen, J.; Qi, H.; Liu, J.; Chen, J.; Zhao, D.; Wang, Z.; Li, X. Neuroprotective potentials of *Panax Ginseng* against Alzheimer's disease: A review of preclinical and clinical evidences. *Front. Pharmacol.* **2021**, *12*, 688490. [[CrossRef](#)] [[PubMed](#)]
105. Liu, M.; Bai, X.; Yu, S.; Zhao, W.; Qiao, J.; Liu, Y.; Zhao, D.; Wang, J.; Wang, S. Ginsenoside Re inhibits ROS/ASK-1 dependent mitochondrial apoptosis pathway and activation of Nrf2-antioxidant response in beta-amyloid-challenged SH-SY5Y cells. *Molecules* **2019**, *24*, 2687. [[CrossRef](#)]
106. Wang, Y.; Kan, H.; Yin, Y.; Wu, W.; Hu, W.; Mingming Wang, M.; Weiping Li, W.; Li, W. Protective effects of ginsenoside Rg1 on chronic restraint stress induced learning and memory impairments in male mice. *Pharmacol. Biochem. Behav.* **2014**, *120*, 73–78. [[CrossRef](#)]
107. Kovac, S.; Angelova, P.R.; Holmström, K.M.; Zhang, Y.; Dinkova-Kostova, A.T.; Abramov, A.Y. Nrf2 regulates ROS production by mitochondria and NADPH oxidase. *Biochim. Biophys. Acta* **2015**, *1850*, 794–801. [[CrossRef](#)]
108. Du, J.; Cui, C.-H.; Park, S.C.; Kim, J.-K.; Yu, H.-S.; Jin, F.-X.; Sun, C.; Kim, S.-C.; Im, W.-T. Identification and characterization of a ginsenoside-transforming  $\beta$ -glucosidase from *Pseudonocardia* sp. Gsoil 1536 and its application for enhanced production of minor ginsenoside Rg2(S). *PLoS ONE* **2014**, *9*, e96914. [[CrossRef](#)] [[PubMed](#)]

109. Lu, C.; Ly, J.; Dong, L.; Jiang, N.; Wang, Y.; Wang, Q.; Li, Y.; Chen, S.; Fan, B.; Wang, F.; et al. Neuroprotective effects of 20(S)-protopanaxatriol (PPT) on scopolamine-induced cognitive deficits in mice. *Phytother. Res.* **2018**, *32*, 1056–1063. [[CrossRef](#)] [[PubMed](#)]
110. Hung, H.S.; Lee, Y.C.; Rhee, Y.K.; Lee, S.Y. Consumer acceptance of ginseng food products. *J. Food Sci.* **2011**, *76*, S516–S522.
111. Meng, X.; Wang, M.; Sun, G.; Ye, J.; Zhou, Y.; Dong, X.; Wang, T.; Lu, S.; Sun, X. Attenuation of A $\beta$ 25–35-induced parallel autophagic and apoptotic cell death by gypenoside XVII through the estrogen receptor-dependent activation of Nrf2/ARE pathways. *Toxicol. Appl. Pharmacol.* **2014**, *279*, 63–75. [[CrossRef](#)]
112. Pan, X.; Matsumoto, M.; Nishimoto, Y.; Ogihara, E.; Zhang, J.; Ukiya, M.; Tokuda, H.; Koike, K.; Akihisa, M.; Akihisa, T. Cytotoxic and nitric oxide production-inhibitory activities of limonoids and other compounds from the leaves and bark of *Melia azedarach*. *Chem. Biodiv.* **2014**, *11*, 1129–1139. [[CrossRef](#)] [[PubMed](#)]
113. Liu, Z.-H.; Ma, R.-J.; Yang, L.; Li, J.-Y.; Hou, B.; Zhou, J. Triterpenoids and iridoids from *Patrinia scabiosaeifolia*. *Fitoterapia* **2017**, *119*, 130–135. [[CrossRef](#)] [[PubMed](#)]
114. Min, S.L.S.; Liew, S.Y.; Chear, N.J.Y.; Goh, B.H.; Tan, W.-N.; Khaw, K.Y. Plant terpenoids as the promising source of cholinesterase inhibitors for anti-AD therapy. *Biology* **2022**, *11*, 307. [[CrossRef](#)] [[PubMed](#)]
115. Dzoyem, J.P.; Tsamo, A.T.; Melong, R.; Mkounga, P.; Nkengfack, A.E.; McGaw, L.J.; Eloff, J.N. Cytotoxicity, nitric oxide and acetylcholinesterase inhibitory activity of three limonoids isolated from *Trichilia welwitschii* (Meliaceae). *Biol. Res.* **2015**, *48*, 57. [[CrossRef](#)] [[PubMed](#)]
116. Sarigaputi, C.; Sommit, D.; Teerawatananond, T.; Pudhom, K. Weakly Anti-inflammatory limonoids from the seeds of *Xylocarpus rumphii*. *J. Nat. Prod.* **2014**, *77*, 2037–2043. [[CrossRef](#)] [[PubMed](#)]
117. Tom, S.; Rane, A.; Katewa, A.S.; Chamoli, M.; Matsumoto, R.R.; Andersen, J.K.; Chinta, S.J. Gedunin inhibits oligomeric A $\beta$ 1–42-induced microglia activation via modulation of Nrf2-NF- $\kappa$ B signaling. *Mol. Neurobiol.* **2019**, *56*, 7851–7862. [[CrossRef](#)] [[PubMed](#)]
118. Wang, J.; Li, L.; Wang, Z.; Cui, Y.; Tan, X.; Yuan, T.; Liu, Q.; Liu, Z.; Liu, X. Supplementation of lycopene attenuates lipopolysaccharide-induced amyloidogenesis and cognitive impairments via mediating neuroinflammation and oxidative stress. *J. Nutr. Biochem.* **2018**, *56*, 16–25. [[CrossRef](#)] [[PubMed](#)]
119. Fakhri, S.; Aneva, I.Y.; Farzaei, M.H.; Sobarzo-Sánchez, E. The neuroprotective effects of astaxanthin: Therapeutic targets and clinical perspective. *Molecules* **2019**, *24*, 2640. [[CrossRef](#)] [[PubMed](#)]
120. Fakhri, S.; Abbaszadeh, F.; Dargahic, L.; Jorjania, M. Astaxanthin: A mechanistic review on its biological activities and health benefits. *Pharmacol. Res.* **2018**, *136*, 1–20. [[CrossRef](#)]
121. Wojtunik-Kulesza, K.A.; Targowska-Duda, K.; Klimek, K.; Ginalska, G.; Jóźwiak, K.; Waksmundzka-Hajnos, M.; Cieśla, L. Volatile terpenoids as potential drug leads in Alzheimer’s disease. *Open Chem.* **2017**, *15*, 332–343. [[CrossRef](#)]
122. Hegazy, M.E.; Ibrahim, A.Y.; Mohamed, T.A.; Shahat, A.A.; El Halawany, A.M.; Abdel-Azim, N.S.; Alsaied, M.S.; Pare, P.W. Sesquiterpene lactones from *Cynara cornigera*: Acetyl cholinesterase inhibition and in silico ligand docking. *Planta Med.* **2016**, *82*, 138–146.
123. Alarcón, J.; Cespedes, C.L.; Muñoz, E.; Balbontin, C.; Valdes, F.; Gutierrez, M.; Astudillo, L.; Seigler, S. Dihydroagarofuranoid sesquiterpenes as acetylcholinesterase inhibitors from Celastraceae plants: *Maytenus disticha* and *Euonymus japonicus*. *J. Agric. Food Chem.* **2015**, *63*, 10250–10256. [[CrossRef](#)]
124. Afifa Zardi-Bergaoui, A.; Znati, M.; Harzallah-Skhiri, F.; Jannet, H.B. Caryophyllene Sesquiterpenes from *Pulicaria vulgaris* Gaertn.: Isolation, structure determination, bioactivity and structure. *Chem. Biodivers.* **2019**, *16*, e1800483.
125. Chougou, R.D.K.; Nguekeu, Y.M.M.; Dzoyem, J.P.; Awouafack, M.D.; Kouamouo, J.; Tane, P.; McGaw, L.J.; Eloff, J.N. Anti-inflammatory and acetylcholinesterase activity of extract, fractions, and five compounds isolated from the leaves and twigs of *Artemisia annua* growing in Cameroon. *Springerplus* **2016**, *5*, 1525. [[CrossRef](#)]
126. Yang, D.-L.; Li, W.; Dong, W.-H.; Wang, J.; Mei, W.-L.; Dai, H.-F. Five new 5,11-epoxyguaiane sesquiterpenes in agarwood “Qi-Nan” from *Aquilaria sinensis*. *Fitoterapia* **2016**, *112*, 191–196. [[CrossRef](#)] [[PubMed](#)]
127. Liu, Y.; Li, J.; Li, D.; Li, X.-M.; Li, D.; Zhou, G.; Xu, K.-P.; Kang, F.-H.; Zou, Z.-X.; Xu, P.-S.; et al. Anti-cholinesterase activities of constituents isolated from *Lycopodium casuarinoides*. *Fitoterapia* **2019**, *139*, 104366. [[CrossRef](#)]
128. Murata, T.; Seldenge, E.; Oikawa, S.; Ageishi, K.; Batkhuu, J.; Sasaki, K.; Yoshizaki, F. Cholinesterase-inhibitory diterpenoids and chemical constituents from aerial parts of *Caryopteris mongolica*. *J. Nat. Med.* **2015**, *69*, 471–478. [[CrossRef](#)] [[PubMed](#)]
129. Senol, F.S.; Ślusarczyk, S.; Matkowski, A.; Pérez-Garrido, A.; Girón-Rodríguez, F.; Cerón-Carrasco, J.P.; den-Haan, H.; Peña-García, J.; Pérez-Sánchez, H.; Domaradzki, K.; et al. Selective in vitro and in silico butyrylcholinesterase inhibitory activity of diterpenes and rosmarinic acid isolated from *Perovskia atriplicifolia* Benth. and *Salvia glutinosa* L. *Phytochemistry* **2017**, *133*, 33–44. [[CrossRef](#)] [[PubMed](#)]
130. Dash, U.C.; Kanhar, S.; Dixit, A.; Dandapat, J.; Sahoo, A.K. Isolation, identification, and quantification of pentylcurcumene from *Geophila repens*: A new class of cholinesterase inhibitor for Alzheimer’s disease. *Bioorg. Chem.* **2019**, *88*, 102947. [[CrossRef](#)]
131. Liu, Y.; Chen, G.; Chen, X.; Chen, S.-X.; Gan, L.-S.; Tao Yuan, T. Colocynthenins A–D, ring-A *seco*-cucurbitane triterpenoids from the fruits of *Citrullus colocynthis*. *J. Nat. Prod.* **2018**, *81*, 2115–2119. [[CrossRef](#)]
132. Wei, J.-C.; Wang, A.-H.; Wei, Y.-L.; Huo, X.-K.; Tian, X.-G.; Feng, L.; Ma, X.-C.; Wang, C.; Huang, S.-S.; Jia, J.-M. Chemical characteristics of the fungus *Ganoderma lucidum* and their inhibitory effects on acetylcholinesterase. *J. Asian Natural Products Res.* **2018**, *20*, 992–1001. [[CrossRef](#)] [[PubMed](#)]

133. Liu, J.-Q.; Peng, X.-R.; Xu-Yang Li, X.-Y.; Li, T.-Z.; Zhang, W.-M.; Shi, L.; Han, J.; Qiu, M.-H. Norfriedelins A-C with acetylcholinesterase inhibitory activity from acerola tree (*Malpighia emarginata*). *Org. Lett.* **2013**, *15*, 1580–1583. [[CrossRef](#)] [[PubMed](#)]
134. Ado, M.A.; Maulidiani, M.; Ismail, I.S.; Ghazali, H.M.; Shaari, K.; Abas, F. Acetylcholinesterase and  $\alpha$ -glucosidase inhibitory compounds from *Callicarpa maingayi*. *Nat. Prod. Res.* **2021**, *35*, 2992–2996. [[CrossRef](#)] [[PubMed](#)]
135. Jamila, N.; Khairuddean, M.; Yeong, K.K.; Osman, H.; Murugaiyah, V. Cholinesterase inhibitory triterpenoids from the bark of *Garcinia hombroniana*. *J. Enzym. Inhib. Med. Chem.* **2015**, *30*, 133–139. [[CrossRef](#)] [[PubMed](#)]
136. Li, H.; Sun, W.; Deng, M.; Qi, C.; Chen, C.; Zhu, H.; Luo, Z.; Wang, J.; Xue, Y.; Zhang, Y. Aperversins A and B, two novel meroterpenoids with an unusual 5/6/6/6 ring from the marine-derived fungus *Aspergillus versicolor*. *Mar. Drugs* **2018**, *16*, 177. [[CrossRef](#)] [[PubMed](#)]
137. Cavalli, A.; Bolognesi, M.L.; Minarini, A.; Rosini, M.; Tumiatti, V.; Recanatini, M.; Melchiorre, C. Multi-target-directed ligands to combat neurodegenerative diseases. *J. Med. Chem.* **2008**, *51*, 347–372. [[CrossRef](#)] [[PubMed](#)]
138. Zhou, J.; Jiang, X.; He, S.; Jiang, H.; Feng, F.; Liu, W.; Qu, W.; Sun, H. Rational design of multitarget-directed ligands: Strategies and emerging paradigms. *J. Med. Chem.* **2019**, *62*, 888–8914. [[CrossRef](#)]
139. Kabir, A.; Muth, A. Polypharmacology: The science of multi-targeting molecules. *Pharmacol. Res.* **2022**, *176*, 106055. [[CrossRef](#)]
140. Lima, E.; Medeiros, J. Marine organisms as alkaloid biosynthesizers of potential anti-Alzheimer agents. *Mar. Drugs* **2022**, *20*, 75. [[CrossRef](#)]
141. Prati, F.; Uliassi, E.; Bolognesi, M. Two disease, one approach: Multitarget drug discovery in Alzheimer's and neglected tropical diseases. *Med. Chem. Comm.* **2014**, *5*, 853–861. [[CrossRef](#)]

**Disclaimer/Publisher's Note:** The statements, opinions and data contained in all publications are solely those of the individual author(s) and contributor(s) and not of MDPI and/or the editor(s). MDPI and/or the editor(s) disclaim responsibility for any injury to people or property resulting from any ideas, methods, instructions or products referred to in the content.